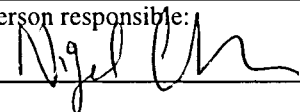


NGU Report 99.032

Carbonate rocks of the Tverrvika area, Beiarn:
potential for white calcite marbles, chemistry,
isotope geochemistry and age.

Report no.: 99.032		ISSN 0800-3416	Grading: Open	
Title: Carbonate rocks of the Tverrvika area, Beiarn: potential for white calcite marbles, chemistry, isotope geochemistry and age.				
Authors: Melezhik, V.A., Gorokhov, I.M., Gjelle. S., Fallick, A.E., Øvereng, O., Sjørdal, T., Gautneb, H.			Client: NGU	
County: Nordland		Commune: Beiarn		
Map-sheet name (M=1:250.000) Bodø		Map-sheet no. and -name (M=1:50.000) 2029 III, Saltstraumen		
Deposit name and grid-reference:		Number of pages: 58..... Price (NOK): 244 Map enclosures: Two		
Fieldwork carried out: 15.08.96-30.11.97	Date of report: 01.05.99	Project no.: 2705.06	Person responsible: 	
Summary: <p>Marbles at Beiarn are a part of the Sokumfjell Group belonging to the Beiarn Nappe Complex in the Uppermost Allochthon of the Nordland Caledonides. The Sokumfjell Group marbles have been subjected to several phases of deformation culminating with amphibolite facies metamorphism. The 1:5, 000 mapping of ca. 1000 m-thick carbonate sequence reveals four different lithofacies of calcite marbles and one composed of diagenetically formed dolomite marble. The calcite marbles exhibit, throughout, different scale rhythmic bedding and textural grading indicating that carbonate material was redeposited by pelagic turbidite system. Both proximal and distal facies have been identified. More than 100 samples were analysed for major and trace elements, acid-soluble Mg and Ca, and 46 samples were analysed for $\delta^{13}\text{C}$, $\delta^{18}\text{O}$ and $^{87}\text{Sr}/^{86}\text{Sr}$. All calcite marbles are enriched in Sr averaging at 2000 ppm. The calcite marbles are characterised by $^{87}\text{Sr}/^{86}\text{Sr}$ ratios ranging between 0.70642 and 0.70999, and $\delta^{13}\text{C}$ values ranging between +1.3 and +8.4‰ PDB. The 'best preserved' samples selected on the basis of their $\delta^{18}\text{O}$ values, and Mn and Sr concentration as well as their ratios, yield average $^{87}\text{Sr}/^{86}\text{Sr}$ values of 0.70662, 0.70698, 0.70727 and 0.70749 for Lithofacies 1, 2, 3 and 4, respectively. Projection of these values along with $\delta^{13}\text{C}$ measurements into $^{87}\text{Sr}/^{86}\text{Sr}$ and $\delta^{13}\text{C}$ calibration curves for the secular variations of seawater suggests that the lithofacies studied were apparently deposited within a 597-608 Ma time interval. White, pure, calcite marbles of Lithofacies 1 were deposited at 608 Ma. They have low contents of SiO_2 and MgO and meet the requirements for industrial use. However, penetrative 440-490 Ma granite magmatism resulted in the formation of ubiquitous, small-scale veins and dikes. Industrial extraction of pure marbles is hardly possible due to inevitable contamination by granite inclusions. The studied area should not be considered for further exploration. A computerised data base for the study includes more than 100 chemical and 46 isotope analyses connected to 1:5,000 digital lithological map.</p>				
Keywords: Marble		Neoproterozoic		Industrial mineral
Strontium		Carbon		Oxygen
Isotopes		Age		Sedimentology

CONTENTS

1.	INTRODUCTION.....	6
2.	TECTONOSTRATIGRAPHIC SECESSION.....	7
3.	INTRUSIVE ROCKS.....	11
4.	DEFORMATION, STRUCTURES AND REGIONAL METAMORPHISM	11
5.	RADIOMETRIC AGE CONSTRAINTS.....	20
6.	LITHOLOGY AND DEPOSITIONAL PALAEOENVIRONMENTS OF THE SOKUMFJELL GROUP MARBLES	21
6.1	LITHOFACIES DESCRIPTION	21
6.2	DEPOSITIONAL ENVIRONMENT	25
7.	PETROGRAPHY OF THE SOKUMFJELL GROUP CARBONATES.....	26
8.	METHODS	27
9.	MAJOR ELEMENT GEOCHEMISTRY	28
10.	CARBON, OXYGEN AND STRONTIUM ISOTOPES	28
11.	THE APPARENT AGE OF THE SOKUMFJELL GROUP.....	46
11.1	STRONTIUM ISOTOPE VARIATIONS.....	47
11.2	CARBON ISOTOPE VARIATIONS.....	49
12.	INCONSISTENCY BETWEEN THE MAP AND THE AGE DATA	50
13.	POTENTIAL OF THE SOKUMFJELL GROUP CARBONATES FOR WHITE MARBLES.....	51
14.	DATA BASE	51
15.	CONCLUSIONS.....	52

FIGURES

Figure 1.	(a) Location map and (b) simplified geological map of the Beiarn area (after Tørudbakken & Brattli 1985, Solli 1990).....	8
Figure 2.	Lithological map of the Tverrvika area, Beiarn (made by S.Gjelle, produced by Sørdal, T.) Throughout the mapped area there are numerous granitic and tonalitic veins and dykes. Only the largest dykes are indicated on the map.	9
Figure 3.	Tectonostratigraphy of the Beiarn Nappe Complex. Tectonostratigraphic units have been defined by the following authors: Sundsfjord by Rutland & Nicholson (1965) and Solli (1990); Sokumfjell Group by Rutland (1959); Stabbursdal and Gråtådal units by Styles (1974); Pallrakken by Bennett (1970) and Solli (1990); Habreså/Stabben and Kovdistind (Govddestinden) unit by Tørudbakken	

	& Brattli (1985), Beiarn Nappe Complex by Rutland & Nicholson (1965). Habreså/Stabben and Kovdistind units was considered by Hollingworth et al. (1960) as Vegdal Group.	10
Figure 4.	Structural map of the Terrvika area, Beiarn, showing structural subareas and axial plane traces (made by S.Gjelle, produced by Sørdal, T.).....	12
Figure 5.	Poles to 105 bedding planes, contoured. Beta axis at 257/18.	13
Figure 6.	All the recorded lineations (L_1 -circles) and small-scale fold axes (F_1 -stars) of the oldest deformation phase, and fold axes (F_2 -triangles) of the second deformation phase.	13
Figure 7.	Structures west of Tarnesodden. Square - boudin axis. Triangles - F_2 axes. Circles - F_1 lineations. Star - axis of small-scale isoclinal fold.	14
Figure 8.	Structural relationships at Lemman. Beta axis (star) defined by seven bedding pole measurements (circles).	15
Figure 9.	Measurements of poles to bedding from the northern half of the area, excluding Lemman. 34 locations, beta axis at 257/15.	15
Figure 10.	Poles to bedding from the southern part of the area. Beta axis (star) at about 262/18. 43 localities..	16
Figure 11.	Bedding poles and lineation from Leiråga-Storliåga. Seven bedding surfaces (circles) are recorded, and one lineation (triangle). Beta axis (star) at 280/16.	16
Figure 12.	Bedding at six scattered locations at Langstiberget. Beta axis (star) at 236/7.	17
Figure 13.	Small-scale isoclinal folds of the F_1 deformation phase.	18
Figure 14.	Vertical, granitic dyke along the fault plane.	19
Figure 15.	Textural characteristics of Lithofacies 1 marbles. (a) Very pure calcite marbles exhibit rhythmic bedding. (b) marble beds subjected to considerable tectonic strain producing marked thinning, which is expressed by the development of nearly blastomylonitic structure. Pen length is 14 cm...22	
Figure 16.	Rhythmically bedded marbles of Lithofacies 2. (a) Impure, grey, rhythmically banded marble. Note that beds are composed of quartz-plagioclase-biotite schist whereas interbeds consist of calcite marble. The lower bedding planes are sharp whereas the upper ones may be both gradational and sharp which is a typical feature of the event beds. (b) Beds and interbeds form interbed-dominated couplets; several couplets are separated by the thicker interbeds and form bedsets.	23
Figure 17.	Millimetre-scale banding in Lithofacies 3marble. Tectonic strain produced marked layer parallel thinning, peaches, swells and boudinage. Coin -2 cm in diameter.	24
Figure 18.	Lithofacies 4. Diagenetically/metamorphically formed bands of dolomite (pale yellow) superimposed on primary bedding. Pen length is 15 cm.	25
Figure 19.	Ca, Mg, SiO ₂ , C _{org} cross-plots for the Sokumfjell marbles.	41
Figure 20.	$\delta^{13}C$, $\delta^{18}O$, Mn/Sr cross-plots for the Sokumfjell marbles.	42
Figure 21.	Oxygen and carbon isotopes versus Mg/Ca ratios for the Sokumfjell marbles. Arrows indicate alteration trends caused by dolomitisation.	43
Figure 22.	Strontium isotope ratios versus $\delta^{13}C$, $\delta^{18}O$, Mn/Sr, Mg/Ca and 1/Sr values. Pink- and blue-shaded areas as well as grey arrows indicate alteration trends.	44
Figure 23.	Stratigraphic variation of $^{87}Sr/^{86}Sr$, $\delta^{13}C$ and $\delta^{18}O$ in carbonates of the Sokumfjell Group. Mean values, indicated as large symbols, are based on the least altered samples (Table 2, see text). Ranges, indicated by small solid symbols, are based on the least altered samples (Table 2). Values for dolomite marbles are indicated by open symbols.	48
Figure 24.	$^{87}Sr/^{86}Sr$ and $\delta^{13}C$ and $\delta^{18}O$ age curves with projections of mean $^{87}Sr/^{86}Sr$ and $\delta^{13}C$ values calculated from the least altered samples of the Sokumfjell Group. Vertical arrowhead lines indicate apparent depositional ages for different lithofacies. The Sr-isotope calibration curve is based on data from Veizer et al. (1983), Asmeron et al. (1991), Derry et al. (1992), Gorokhov et al. (1995), Kaufman & Knoll (1995), Nicholas (1996) and Denison et al. (1998). The C-isotope calibration curve is based on data from Derry et al. (1992), Kaufman & Knoll (1995) and Azmy et al. (1998). The new age for the Cambrian-Ordovician boundary is based on Davidek et al. (1998).49	
Figure 25.	Granite inclusions in Lithofacies 3 marbles.	52

TABLES

<i>Table 1.</i>	<i>Chemical composition of carbonate rocks of the Beiarn area.</i>	<i>29</i>
<i>Table 2.</i>	<i>Chemical and isotope composition of carbonate rocks from the Beiarn area.</i>	<i>37</i>

APPENDIX

<i>Appendix 1.</i>	<i>Variation in soluble MgO.</i>
<i>Appendix. 2</i>	<i>Variation in soluble CaO.</i>

1. INTRODUCTION

This report will show the results obtained within the project 2705.06 entitled 'Carbonate formations of the Beiarn area' which is a part of a larger, multidisciplinary project 2705.00 'Carbonate formations of Norway: from basic research to industry'. The carbonate rocks developed in the vicinity of a small village Beiarn (Figs. 1 & 2), were chosen as one of the objects which have been considered to have a certain potential for good quality white calcite marbles which can be used for the paper industry. The results shown in this report have been obtained during a three year period from 15.08.96 to 30.11.97.

The main objectives were:

- 1:20,000 geological map;
- 1:20,000 structural map;
- defining local and regional lithostratigraphical marker horizons (diagenetic and syngenetic dolostones, Leivset-type pink marbles, iron formations, etc.);
- stratigraphic/tectonostratigraphic subdivisions of carbonate formations;
- stratigraphic nomenclature of available carbonate formations based on the Norwegian Stratigraphic Code (1986);
- 1:20,000 lithological map (distribution of dolostone-limestone, pure-impure carbonates, banded-massive carbonates, dykes, veins, etc.);
- 1:50,000 geochemical maps (SiO_2 , Fe_{tot} , C_{org} , MgO/CaO , $\delta^{13}\text{C}$, $\delta^{18}\text{O}$);
- geochemical and mineralogical composition of main carbonate units;
- depositional environments;
- depositional ages;
- defining areas for follow-up work with a high potential for industrial use (fillers, dimension stones, cement industry, agriculture, etc.);
- data base (this includes mineralogical and geochemical compositions of carbonate rocks assigned to the digital map).

The project was carried out by the Geological Survey of Norway (NGU) jointly with the Institute of Precambrian Geology and Geochronology (IGGD) in St. Petersburg, Russia, and

the Scottish Universities Research and Reactor Centre (SURRC) in East Kilbride, Glasgow, Scotland. The field work, XRF-major and trace elements analyses were supported by NGU (Project 2705.06). Whole-rock carbon and oxygen isotope analyses were supported by NGU and SURRC. Rb-Sr and strontium isotope analyses were financed by NGU and partly by IGGD.

2. TECTONOSTRATIGRAPHIC SUCCESSION

The marble succession studied is a part of a thick unit within a group known from earlier literature as the Sokumfjell Group (Fig. 1, 3, Rutland 1959). This group together with the Stabbursdal (Styles 1974), Sundsfjord/Pallrakken (Solli 1990), Gråtådal (Styles 1974), Habreså/Stabben and Kovdistind (Tørudbakken & Brattli 1985) tectonostratigraphic units were considered to form the Beiarn Nappe Complex in the Uppermost Allochthon of the Nordland Caledonides (Fig. 1, 3, Rutland & Nicholson 1965). The Beiarn Nappe Complex forms a large synformal structure bounded by thrust boundaries.

The Stabbursdal, Sundsfjord/Pallrakken units tectonically underlie the Sokumfjell Group. They consist of mica schists and gneisses, augen gneisses, and strongly migmatized gneisses (Tørudbakken & Brattli 1985, Solli 1990). The Sokumfjell Group, which lies tectonically above the Sundsfjord/Pallrakken groups, is believed to occupy the same tectonostratigraphic position as the Gråtådal unit in the east (Tørudbakken & Brattli 1985). Both, the Sokumfjell and Gråtådal units, consist of calcite marbles with bands of dolomite marbles and mica schists. Matrix-supported conglomerates, quartzite, and calc-silicate schists are less developed, and have only been documented in the Sokumfjell Group. The juxtaposition of the Sokumfjell marble and the Gråtådal marble has never been confirmed in the field (Solli, pers. comm. 1999). The tectonostratigraphically overlying rock complexes are the Habreså and Stabben units (Fig. 1, 3). They are nearly symmetrically exposed on both sides of the Kovdistind unit, and both are made up of homogeneous mica schist with minor beds of

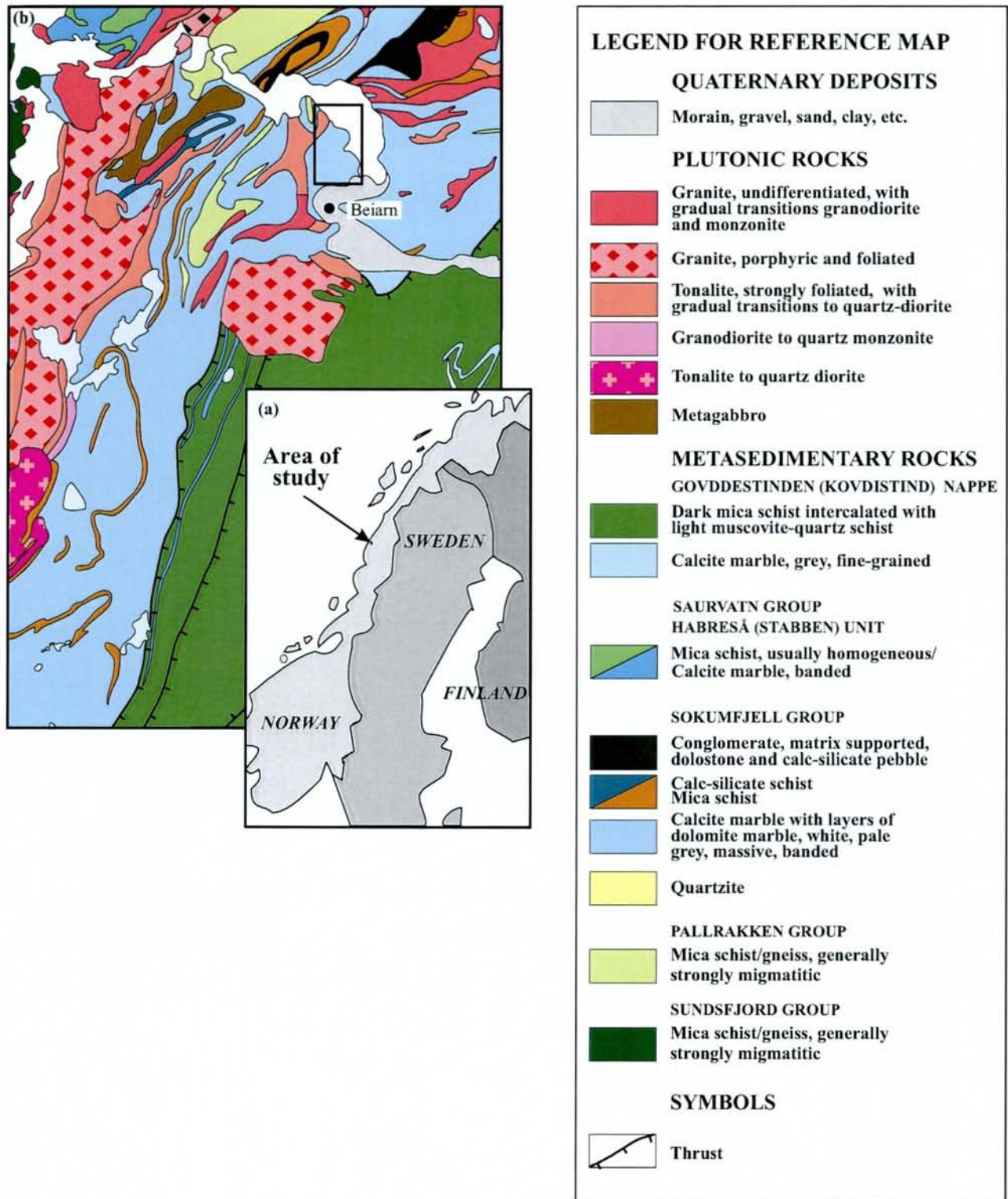


Figure 1. (a) Location map and (b) simplified geological map of the Beiarn area (after Torudbakken & Brattli 1985, Solli 1990).

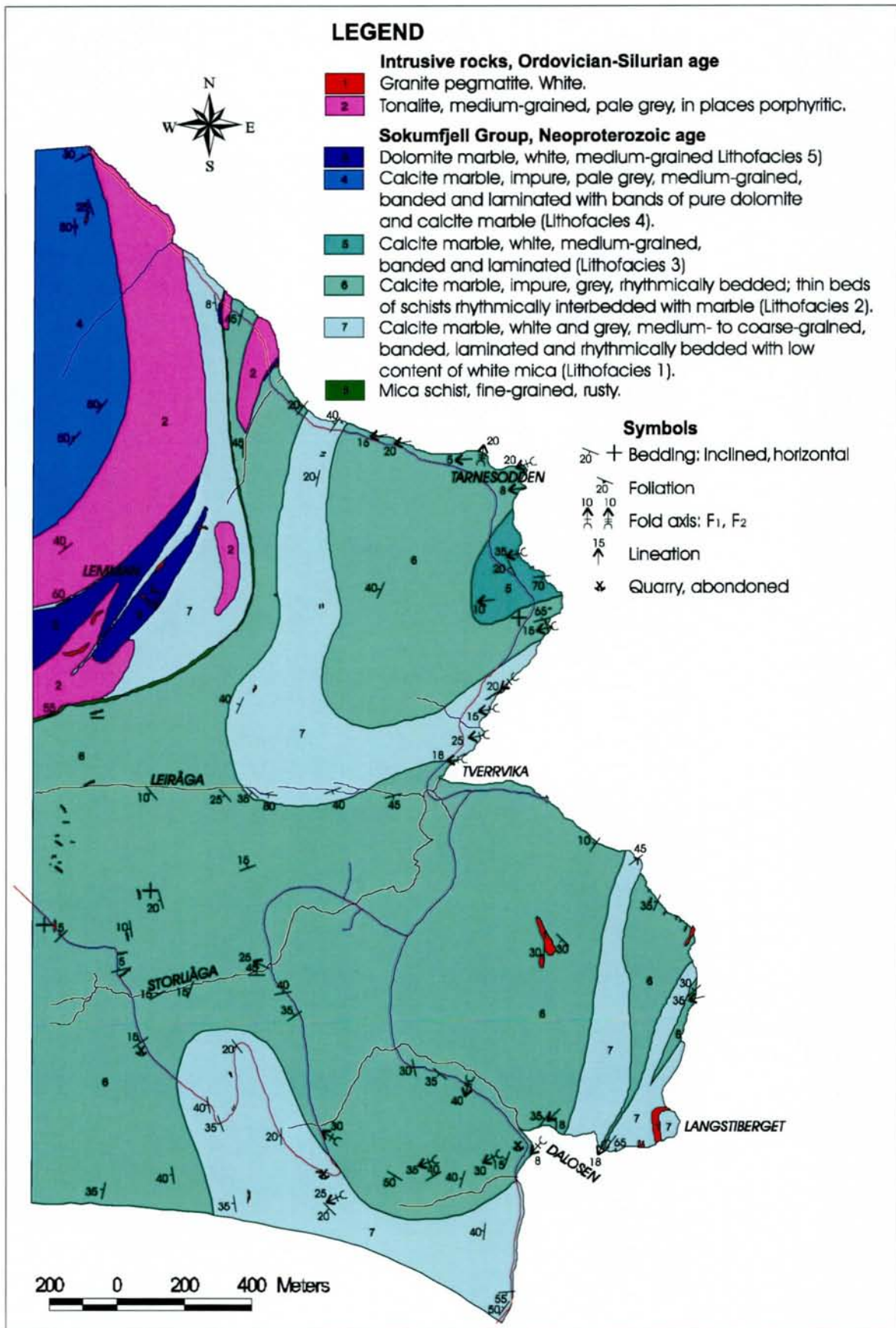


Figure 2. Lithological map of the Tverrvika area, Beiarn (made by S.Gjelle, produced by Sordal, T.) Throughout the mapped area there are numerous granitic and tonalitic veins and dykes. Only the largest dykes are indicated on the map..

Beiarn Nappe Complex	Tectonostratigraphy	Lithology	Method	Age, Ma	$^{87}\text{Sr}/^{86}\text{Sr}_1$	MSWD	References to age	
	Kovdistind unit (Govddestinden Nappe)	Høgtind granite	Rb-Sr _{wr}	440±30	0.7089± 6	4.05	Tørudbakken & Brattli 1985	
		Harefjell diorite gneiss	Rb-Sr _{wr}	470±59	0.7080± 8	0.59	Cribb 1981	
		Harefjell quartz-monzonite gneiss	Rb-Sr _{wr}	495±14	0.7094± 6	2.29	Cribb 1981	
	Habreså/ Stabben unit	Pelitic schist	Rb-Sr _{wr}	606±99	0.724	70.4	Tørudbakken & Brattli 1985	
		Schist	Rb-Sr _{wr}	658±29	-	-	Styles 1978	
		Pelitic schist	Rb-Sr _{wr}	690±63	0.720	18.5	Tørudbakken & Brattli 1985	
	Sokumfjell/ Gråtådal unit	Calcite marbles	$^{87}\text{Sr}/^{86}\text{Sr}$ vs. $\delta^{13}\text{C}_{\text{carb}}$	600	0.70677	-	-	This study
	Stabursdal/ Pallrakken/ Sundsford Group	Gneiss	Rb-Sr _{wr}	858±61	-	-	-	Styles 1978

Figure 3. *Tectonostratigraphy of the Beiarn Nappe Complex. Tectonostratigraphic units have been defined by the following authors: Sundsfjord by Rutland & Nicholson (1965) and Solli (1990); Sokumfjell Group by Rutland (1959); Stabursdal and Gråtådal units by Styles (1974); Pallrakken by Bennett (1970) and Solli (1990); Habreså/Stabben and Kovdistind (Govddestinden) unit by Tørudbakken & Brattli (1985), Beiarn Nappe Complex by Rutland & Nicholson (1965). Habreså/Stabben and Kovdistind units was considered by Hollingworth et al. (1960) as Vegdal Group.*

marble. Based on these facts they were considered to be correlated (Tørudbakken & Brattli 1985). The uppermost tectonostratigraphic level in the study area is the Kovdistind unit which discordantly cuts with a thrust both the Habreså and Stabben units (Fig. 1, 3). The unit consists largely of a finely banded light and dark mica schist sequence (Tørudbakken & Brattli 1985).

3. INTRUSIVE ROCKS

The Harefjell diorite complex, Høgtind granite and Høgfjell gabbro are the major masses of intrusive rocks in the area of study (Fig. 1). The Harefjell diorite complex occurs in the core of a synformal structure termed the Beiarn Nappe Complex (Rutland & Nicholson 1965). A series of rock-types have been recognised within the Harefjell diorite complex (Rutland 1959, Brattli & Tørubakken 1987, Solli 1990). These are porphyric and foliated granite, quartz-diorite, granodiorite, monzonite and tonalite. Large portion of granite occurs as porphyric varieties. Some granites, diorites and tonalites are strongly foliated indicating their emplacement between the the F_1 and F_2 phases of folding. The Høgtind granite massif occurs east of the Harefjell diorite complex. This massif is post-metamorphic and cuts the thrust boundary between the Habreså/Stabben and Kovdistind units as well as the boundary between the Habreså and Skumfjell units (Brattli & Tørubakken 1987, Solli 1990). The massif is largely made up of porphyric granit with minor development of granodiorite and monzonite (Brattli & Tørubakken 1987, Solli 1990).

4. DEFORMATION, STRUCTURES AND REGIONAL METAMORPHISM

All supracrustal rocks of the Beiarn Nappe Complex have been affected by three phases of deformation (F_1 , F_2 and F_3 , Rutland & Nicholson 1965, Styles 1974, Tørubakken & Brattli 1985) although a pre- F_1 phase of folding has been recognised in the Stabbursdal unit (Styles 1978). Folds belonging to the first phase of deformation show a different pattern in the Kovdistind unit compared to the underlying rocks (Tørubakken & Brattli 1985) while the F_2 and F_3 folds have affected all units in the same manner.

In the Tverrvik area, structures of at least two of these phases of deformation are present (Fig. 4). This is in accord with the description by Rutland (1959) of the Sokumvatn area situated about 15 km to the southwest. Rutland described an early deformation which produced recumbent, ENE–WSW-trending isoclinal folds, and a later fold deformation with approximately N–S axes.

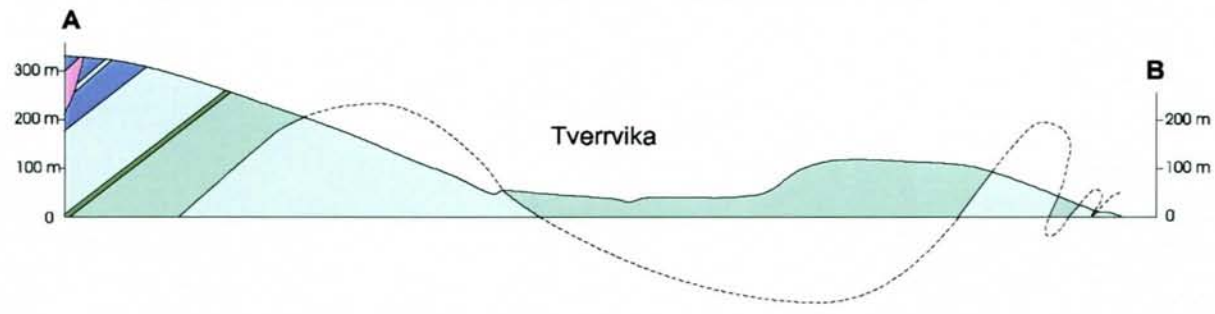
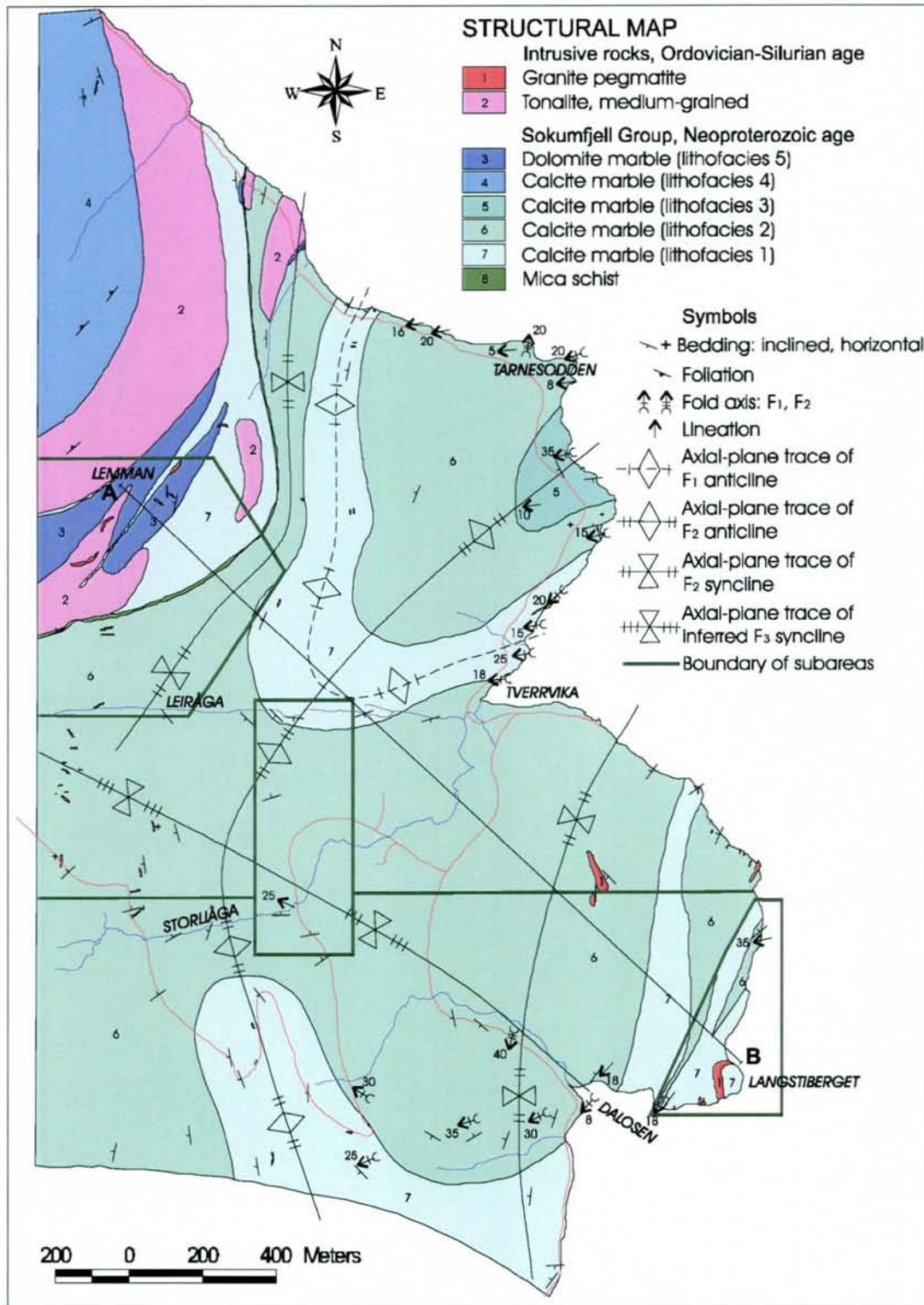


Figure 4. Structural map of the Tverrvika area, Beiarn, showing structural subareas and axial plane traces (made by S.Gjelle, produced by Sordal, T.).

Fig. 5 shows all the measurements of bedding surfaces from the area plotted as poles and contoured in an equal-area projection. The bedding poles define a broad band along a great circle indicating a fold axis plunging gently WSW.

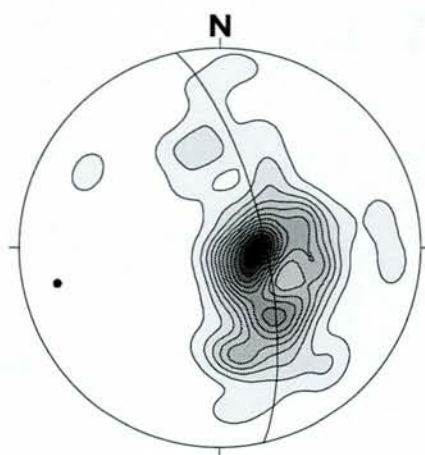


Figure 5. Poles to 105 bedding planes, contoured. Beta axis at 257/18.

There is also a concentration of small-scale fold axes and other lineations in this direction as shown in Fig. 6.

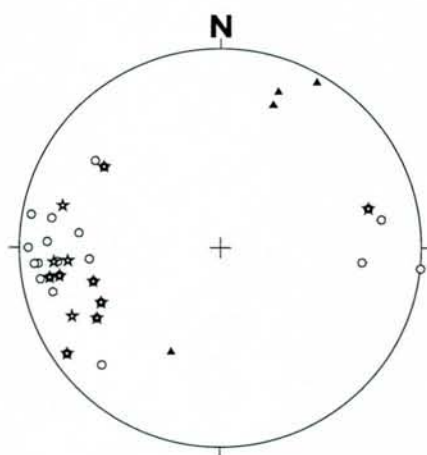


Figure 6. All the recorded lineations (L_1 -circles) and small-scale fold axes (F_1 -stars) of the oldest deformation phase, and fold axes (F_2 -triangles) of the second deformation phase.

Along the beach just west of Tarnesodden there is a locality where granitic pegmatite dykes are cross-cutting isoclinal folds of the first deformation phase. These dykes are boudinaged and were subsequently deformed by NNE-plunging folds which are inferred to relate to the second phase of deformation. An early lineation trending almost east-west and supposedly related to the F_1 deformation is also seen at this location. Fig. 7 shows the structural relationships in an equal-area projection. The F_2 axes (triangles) are roughly parallel to the long axis of the boudins (square). The folded lineation (circles) is approximately parallel to the axis of the isoclinal F_1 folds.

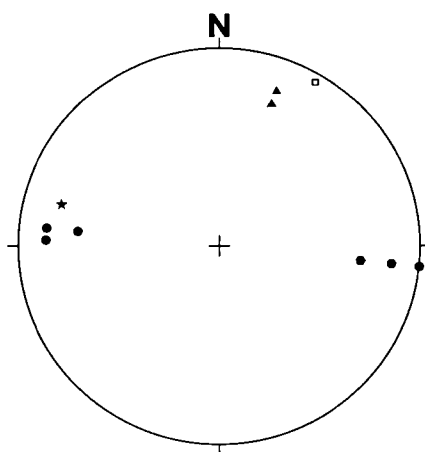


Figure 7. *Structures west of Tarnesodden. Square - boudin axis. Triangles - F_2 axes. Circles - F_1 lineations. Star - axis of small-scale isoclinal fold.*

At Lemman, about 1 km southwest of Tarnesodden, the bedding attitude at seven scattered localities vaguely defines a possible fold axis plunging gently to the north-northeast (Fig. 8). This is the only area where the F_2 axial trend is shown by the bedding. The beta axis at 020/15 agrees well with the F_2 trend and plunge in the region and is also in agreement with the measured fold axes of the second generation of folds as seen at Tarnesodden (Fig. 7).

In order to obtain a better defined girdle and beta axis, the poles to bedding in the northern and southern areas are plotted in two separate diagrams in Fig. 9 and 10. In addition, bedding measurements from the subareas at Lemman, Leiråga-Storliåga and Langstiberget are plotted separately (Fig. 8, 11 and 12). The locations of these different structural areas are shown in Fig. 4.

At Langstiberget, six scattered locations give a pretty well defined axis plunging at approximately 7° to the southwest (236°). At Leiråga-Storliåga, the bedding at seven different

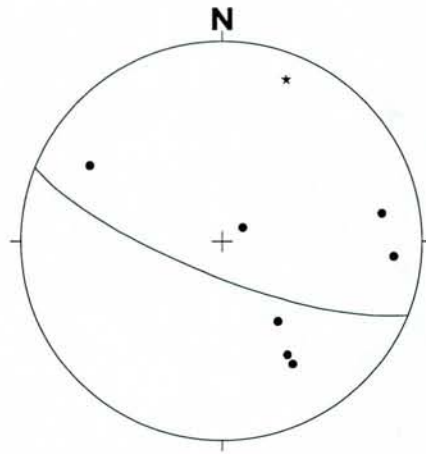


Figure 8. Structural relationships at Lemman. Beta axis (star) defined by seven bedding pole measurements (circles).

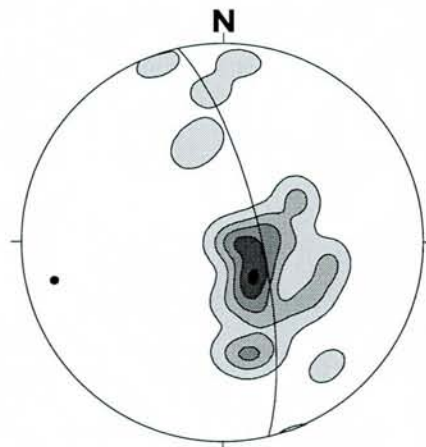


Figure 9. Measurements of poles to bedding from the northern half of the area, excluding Lemman. 34 locations, beta axis at 257/15.

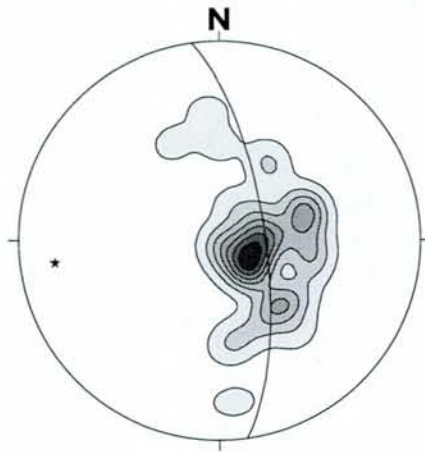


Figure 10. Poles to bedding from the southern part of the area. Beta axis (star) at about 262/18. 43 localities.

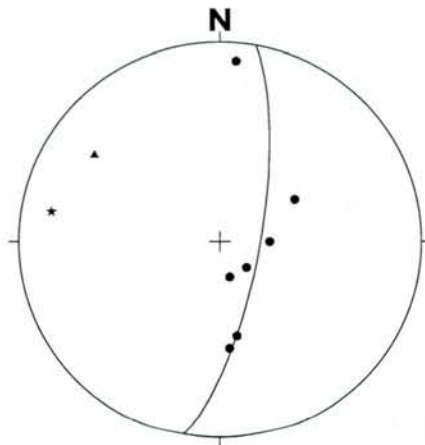


Figure 11. Bedding poles and lineation from Leiråga-Storliåga. Seven bedding surfaces (circles) are recorded, and one lineation (triangle). Beta axis (star) at 280/16.

localities defines a beta axis plunging 16° to the west-northwest (280°). This is roughly the same trend and plunge as shown by the lineations and small-scale fold axes of the F_1 deformation phase (Fig. 6).

Fig. 9 and 10, which cover larger areas than in the cases of Fig. 8, 11 and 12, show that the poles to bedding are distributed in a broad band. These bands do not define the beta axis any better than in Fig. 5 where all of the bedding measurements are plotted.

The small-scale folds are usually of isoclinal type (Fig. 13), and their axes are plunging in a westerly direction. This also holds for most of the folds of a more open type that have been observed in different parts of the area. Only the fold west of Tarnesodden (Fig. 7) and one fold in a road-cut about 200 m northwest of Dalosen are related to the more open folding of the second generation. The fold near Dalosen is plunging at about 40° towards south-southwest, and its axial-plane dips steeply to the southwest.

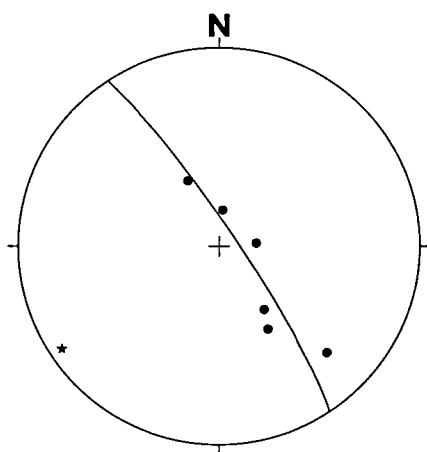


Figure 12. Bedding at six scattered locations at Langstiberget. Beta axis (star) at 236/7.

A NW-SE section across the F_2 -folds is shown in Fig. 4. The sketch shows open folds with axial planes dipping steeply WNW. In the southern part of the map these axial planes are turning towards the southeast, a feature which may be ascribed to a third phase of deformation.

The suggested axial plane traces of the larger, mappable folds are shown in Fig. 4. The map shows the influence of the inferred third phase of open folding with an axial plane trace trending roughly WNW-ESE. This phase of deformation has so far not been confirmed by direct measurements of any small-scale structures.

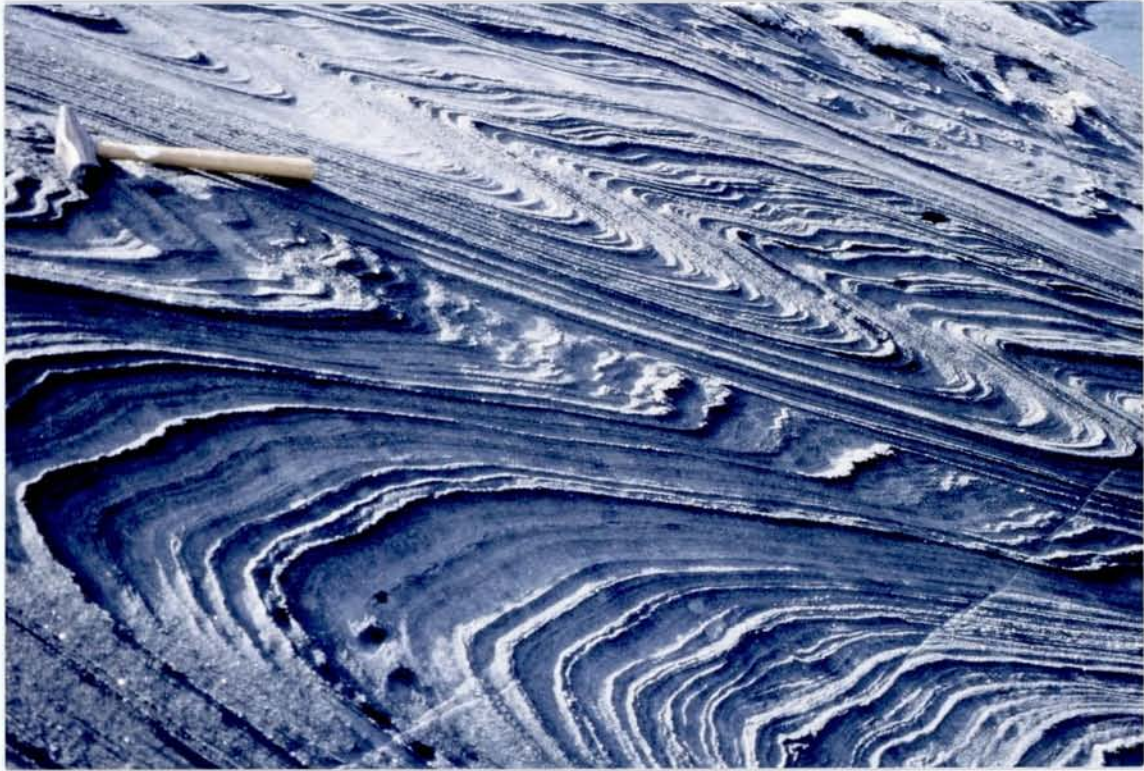


Figure 13. Small-scale isoclinal folds of the F_1 deformation phase.

Based on the lithological succession as defined by the mapping and supported by the chemical (isotope) analyses, the rocks are younging through the fold structure from Kakvika to the core of the F_2 fold just south of Tarnesodden.

A few small-scale faults have been observed in the area. One of them is shown in Fig. 14. A granitic dyke has intruded along the NW-SE-striking, vertical fault plane at this locality,. Dyke intrusion along faults is a common feature in the area. All faults that have been observed are dextral wrench faults.



Figure 14. Vertical, granitic dyke along the fault plane.

The main mineral association in all units underlying the Kovdistind unit have grown during F_1 deformation of kyanite-sillimanite grade (main metamorphism) and define S_1 foliation. In the Kovdistind unit the main schistosity defined by biotite, muscovite, garnet (\pm staurolite) was developed during the F_2 deformation. Therefore the main metamorphism is of garnet-biotite \pm staurolite grade are related to F_2 deformation. Based on these facts the boundary between the Kovdistind unit and the underlying Habreså/Stabben units has been defined as a thrust contact due to early emplacement of Kovdistind unit during a late stage of F_1 folding (Tørudbakken & Brattli 1985). However, since F_2 all the units shared a common later deformation and metamorphic history.

5. RADIOMETRIC AGE CONSTRAINTS

Published Rb-Sr whole-rock ages, which have been obtained for supracrustal rocks of the Beiarf Nappe Complex and spatially related intrusive rocks, are summarised in Fig. 3. The oldest age of 858 ± 61 Ma was reported from the Venset Gneisses of the Stabbursdal unit (Styles 1978). This age was considered to reflect the time of an isotopic homogenisation event related to a high grade metamorphism.

Two dates of 606 ± 99 and 690 ± 63 Ma obtained from pelitic schists of the Kovdistind unit were considered to reflect Neoproterozoic age of these rocks. Similar date of 658 ± 29 Ma was measured from the schist of the Vegdal Group (Styles 1978), which has been redefined and divided into the Habreså/Stabben and Kovdistind units (Tøruðbakken & Brattli 1985, Fig. 3). Taylor (cited in Cribb 1981) suggested that the Rb-Sr data on the Vegdal Group schist is a diagenetic age.

Deformed quartz-monzonite and tonalite of the Harefjell diorite complex yielded 495 ± 14 and 470 ± 59 Ma, respectively (Cribb 1981). These dates were considered as the age of the intrusion providing time constraints between the F_1 and F_2 phases of folding.

The date of 440 ± 30 Ma reported from the undeformed, post-metamorphic Høgtind granite was interpreted as the age of intrusion (Tøruðbakken & Brattli 1985). This suggests that the S_2 foliation and F_2 folding as well as the Sokumfjell-Habreså-Stabben-Kovdistind tectonostratigraphy was established prior to 440 ± 30 Ma. The 397 ± 36 Ma age obtained from the Kovdistind unit is thought to be related to low-grade metamorphic alterations (Tøruðbakken & Brattli 1985).

6. LITHOLOGY AND DEPOSITIONAL PALAEOENVIRONMENTS OF THE SOKUMFJELL GROUP MARBLES

6.1 Lithofacies description

The selected area of 4 km north of Beiarn (Fig. 1) has been mapped on scale 1:5000 in accordance with the main objectives specified in **INTRODUCTION**. The mapping revealed a number of lithological varieties of marbles folded in a complex structure with an inferred tectonostratigraphic thickness of more than 1000 m (Fig. 2, Appendix 1).

All marbles are deformed, metamorphosed and recrystallised under P-T conditions of amphibolite facies, which obliterated primary sedimentological features. The bed thickness of the layered sequence has been subjected to considerable tectonic strain producing marked thinning of the sequence. This is also shown by the observation on ptygmatitic veins, which are strongly folded. These veins themselves, however, can be observed to cut strongly deformed (thinned) layers, and thus the strains shown by the ptygmatitic veins only indicate a phase of the late strain history. However, in places, sedimentary layering has largely been preserved. The marble succession is composed of several lithological varieties of both calcite and dolomite marbles (Fig. 2, Appendix 1), which are assigned to five lithofacies and briefly characterised below.

Lithofacies 1 is represented by a relatively pure, white to pale grey, medium- to coarse-grained, calcite marble which composes one or two 50 to 300 m-thick folded units (Fig. 2). Lithofacies 1 is characterised by millimetre- to centimetre-thick banding and contains very small amount of siliciclastic material. Very pure calcite marbles exhibit rhythmic bedding (Fig. 15a). This is a two-member rhythm expressed by a rhythmic alternation of layers which differ in terms of siliciclastic components and C_{org} content. In places marble beds were subjected to considerable tectonic strain producing marked thinning, which is expressed by the development of nearly blastomylonitic structure (Fig. 15b).

Lithofacies 2 is an impure, grey, banded, marble rhythmically interbedded with layers of calcareous quartz-muscovite-biotite schist. This lithofacies makes up the bulk of the succession within the mapped area. Lithofacies 2 exhibits rhythmical bedding (Fig. 16a). It

has been accepted that “in an alternation of different beds, weathering-resistant beds are described as beds or layers, while less resistant beds may be called interbeds or interlayers” (Ensele et al. 1991, p. 3). In the studied sequence beds are composed of quartz-plagioclase-biotite schist. The observed bed thickness varies from 0.5 to 12 cm though it has been largely overprinted by metamorphic thinning as indicated by the development of pygmatitic veins. The lateral extent of beds ranges from a few meters to a few tens of meters. Beds are separated from each other by thicker (2-5 cm) interbeds of calcite marble.

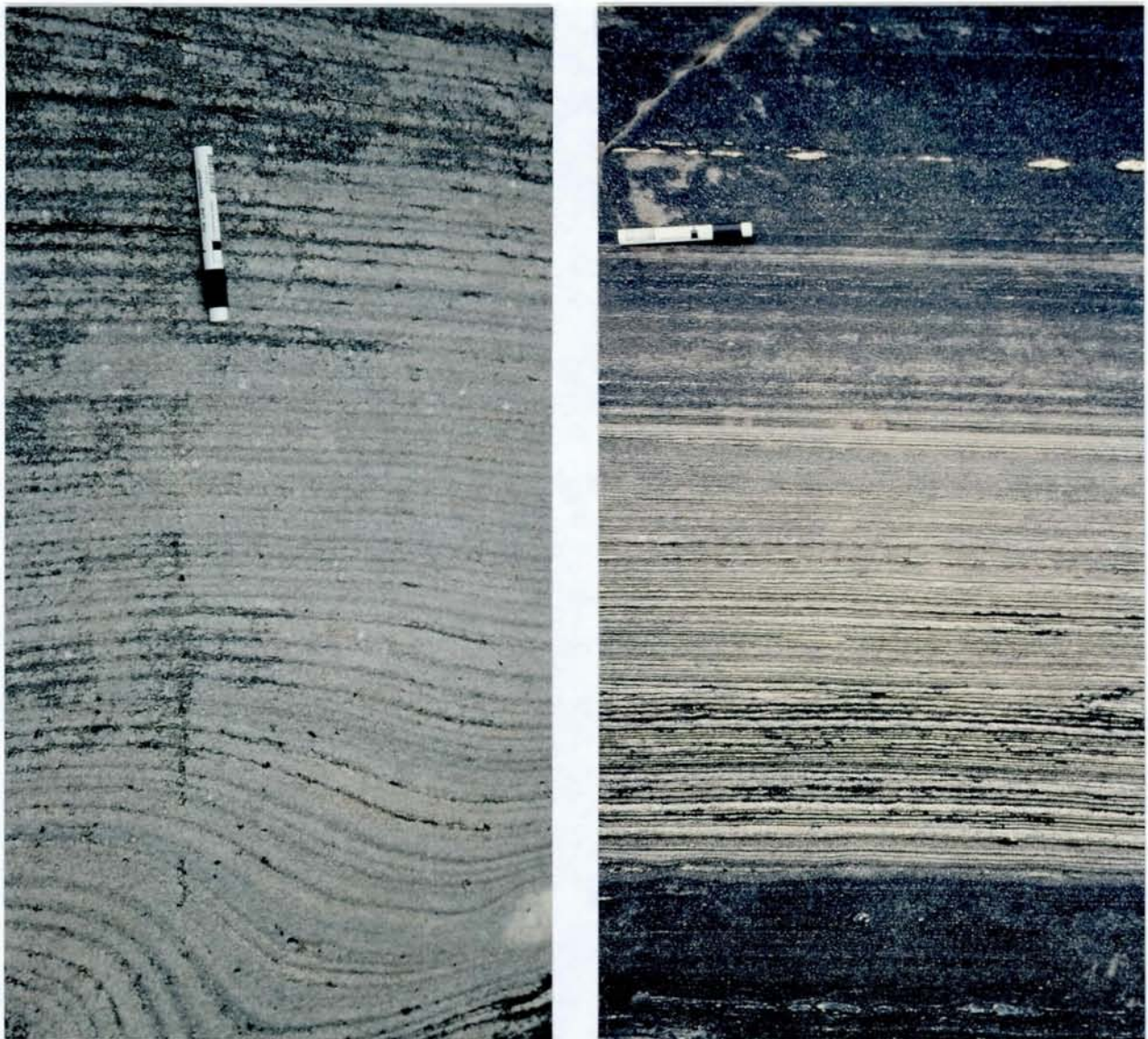


Figure 15. *Textural characteristics of Lithofacies 1 marbles. (a) Very pure calcite marbles exhibit rhythmic bedding. (b) marble beds subjected to considerable tectonic strain producing marked thinning, which is expressed by the development of nearly blastomylonitic structure. Pen length is 14 cm.*

The lower bedding planes are sharp whereas the upper ones may be both gradational and sharp, which is a typical feature of the event beds (Seilacher & Aigner 1991). Beds and intercalations form interbed-dominated couplets. In places, several couplets are separated by the thicker interbeds and form bedsets (Fig. 16b). The graded bedding clearly indicates way-up of the sequence.



Figure 16. *Rhytmically bedded marbles of Lithofacies 2. (a) Impure, grey, rhytmically banded marble. Note that beds are composed of quartz-plagioclase-biotite schist whereas interbeds consist of calcite marble. The lower bedding planes are sharp whereas the upper ones may be both gradational and sharp which is a typical feature of the event beds. (b) Beds and interbeds form interbed-dominated couplets; several couplets are separated by the thicker interbeds and form bedsets.*

Lithofacies 3 is composed of a white, thinly banded, medium-grained, pyrite-bearing, calcite marble, which has minor development in the north-eastern part of the area where it forms a core of the small synform (Fig. 4). *Lithofacies 4* is characterised by millimetre-scale banding. However the scale of primary bedding and lamination cannot be reconstructed as they were subjected to considerable tectonic strain producing marked layer parallel thinning (Fig. 17).



Figure 17. *Millimetre-scale banding in Lithofacies 3 marble. Tectonic strain produced marked layer parallel thinning, peaches, swells and boudinage. Coin -2 cm in diameter.*

Lithofacies 4 consists of an impure, pale grey, banded to laminated, fine-grained, calcite marble interbedded with 1 to 2 cm-thick layers of pure calcite and dolomite marbles. *Lithofacies 4* is only locally developed in the south-eastern and north-western sides of the mapped area.

Lithofacies 4 calcite marbles are characterised by bedding which was essentially modified during diagenesis/ metamorphism. This resulted in the development of dolomite bands which are superimposed on the sedimentary bedding. Thus, a palaeoenvironmental interpretation of *Lithofacies 4* marbles hampers by both diagenetic transformation and tectonic thinning of primary sedimentological features (Fig. 18).

Lithofacies 5 is composed of dolomite marble which is bound to the contact zone between tonalite intrusion and calcite marbles in the north-western corner of the mapped area (Fig. 2). The dolomite marble occur as a series of lenses with unknown sizes due to limited exposures. Dolomite

marbles are usually fine-grained, structureless rocks.

6.2 Depositional environment

The dominant primary structure in most studied carbonates is rhythmic bedding. Although the true scale of the bedding cycles can hardly be estimated however it is clear that the bedding cycles of Lithofacies 2 calcite marbles were >10 centimetre-thick prior to metamorphic thinning. This scale of bedding cycles is important features of nearly all pelagic carbonate sequences (e.g., Scholle et al. 1983).



Figure 18. *Lithofacies 4. Diagenetically/metamorphically formed bands of dolomite (pale yellow) superimposed on primary bedding. Pen length is 15 cm.*

Rhythmic bedding may be caused by fluctuation in depositional environment (Scholle et al. 1983): (i) variations in terrigenous input, (ii) surface productivity/dissolution rate, (iii) current velocity, (iv) water depth. Alternatively, the rhythmic bedding may be caused by redeposition of shelf/slope carbonates by turbidite currents.

Despite of intensive metamorphic overprints numerous beds of the Lithofacies 2 carbonates exhibit well preserved graded bedding and can be clearly identifiable as turbidites (Fig. 16). Thus, the data available indicate that the rhythmic bedding was caused by redeposition.

The sedimentological characteristics of the Lithofacies 1 and 3 calcite marbles have some resemblance with ancient undisturbed slope sediments described in details in numerous publications (e.g., Wilson 1969, Cook & Enos 1977, Cook & Mullins 1983). However Lithofacies 1 and 3 are separated by the carbonate turbidites of Lithofacies 2 which form the bulk of the mapped area. Thus, it is difficult to reconcile the two mutually exclusive environments repeated within a short time interval. Given the fact that, in places, the textural grading has also been observed in the Lithofacies 1 carbonates (Fig. 15a), and that many younger, unmetamorphosed, well-bedded, pelagic carbonate sequences reported from elsewhere contain significant amount of redeposited material which cannot be easily recognised (Scholle et al. 1983), we suggest that all group carbonates apparently belong to the same pelagic turbidite system(s). The only possible difference between larger-scale bedding cycles of Lithofacies 2 and smaller ones of Lithofacies 1 and 3 is that the former indicate a relatively proximal facies whereas the latter belong to a more distal facies. However, if tectonic strain caused differential thinning of Lithofacies 1 and 3 then no reliable difference can be inferred between them and Lithofacies 2 in terms of depositional environments.

7. PETROGRAPHY OF THE SOKUMFJELL GROUP CARBONATES

Carbonate rocks underwent amphibolite facies metamorphism which resulted in the development of granoblastic texture. Calcite marbles are characterised by calcite-(±dolomite)-diopside-quartz-plagioclase-muscovite-graphite paragenesis. Calcite forms isometric crystals with size ranging from 1 to 4 mm. Diopside occurs in a form of poikiloblasts filled with quartz. Diopside is characterised by irregular shape and highly variable crystal sizes. Graphite is a minor mineral though it has been detected in every sample. It occurs as small flakes sizing from 0.005 x 0.02 to 0.01 x 0.15 mm. Pyrite has been constantly observed in the studied carbonate rocks in a form of tiny (0.01-0.3 mm) euhedral crystals. Rutile is present as an accessory mineral.

Muscovite, graphite and pyrite are preferentially accumulated within layers enriched in siliciclastic material. Plagioclase has only been detected within such layers whereas quartz is

relatively evenly distributed in carbonate groundmass. Flakes of graphite and muscovite exhibit no preferential orientation.

Dolomite marbles are composed of dolomite(\pm calcite)-diopside-quartz-muscovite-graphite paragenesis. Dolomite occurs as isometric crystals with size ranging from 0.5 to 1.5 mm. The geometry and sizes of other minerals appear to be similar to those observed in the calcite marble paragenesis. The siliciclastic components in dolomite marbles are represented by quartz with very limited content of plagioclase and diopside.

8. METHODS

Whole-rock oxygen and carbon isotope analyses were carried out at the Scottish Universities Research and Reactor Centre using the phosphoric acid method of McCrea (1950) as modified by Rosenbaum & Sheppard (1986) for operation at 100 °C. Carbon and oxygen isotope ratios were measured on a VG SIRA 10 mass spectrometer. Calibration to international reference material was through NBS 19 and precision (1σ) for both isotope ratios is better than $\pm 0.2\%$. Oxygen isotope data were corrected using the fractionation factor 1.00913 recommended by Rosenbaum & Sheppard (1986) for dolomites. The $\delta^{13}\text{C}$ data are reported in per mil (‰) relative to V-PDB and the $\delta^{18}\text{O}$ data in ‰ relative to V-SMOW.

Whole-rock strontium and rubidium isotope analyses were carried out at the Institute of Precambrian Geology and Geochronology of the Russian Academy of Sciences (St. Petersburg) using the method which is described in detail by Gorokhov et al. (1995). Strontium and rubidium isotope ratios were measured on a MAT-261 mass spectrometer. Calibration to international reference material was through SRM-987 and precision (2σ) for both isotope ratios is better than ± 0.00007 .

The major and trace elements were analysed by X-ray fluorescence spectrometry at NGU using a Philips PW 1480 X-ray spectrometer. The accuracy (1σ) is typically less than 2% of the oxide present (SiO_2 , Al_2O_3 , MgO , CaO). The analytical uncertainties (1σ) for Sr, MnO and Fe_2O_3 are better than ± 5.5 ppm, $\pm 0.01\%$ and $\pm 0.06\%$, respectively.

9. MAJOR ELEMENT GEOCHEMISTRY

One hundred and twenty three samples were analysed for major and trace elements, and one hundred and three of them for acid-soluble MgO and CaO. Table 1 is a summary of trace and major element data. Chemically the calcite marbles approximates to a sandy limestone whereas the dolomite marbles to a pure dolostone though a few samples exhibit high impurity.

The calcite marbles are characterised by a very small concentration of total MgO ranging from 0.1 to 3.4% and averaging at 0.53 ± 0.46 (Fig. 19). However, acid-soluble MgO shows much less abundances, $0.37 \pm 0.27\%$ on average, ranging from 0.06 to 2.2%. This indicates that ca. 70% of the total MgO is bound into silicates. The low MgO abundances suggest that limestones were subjected to a limited degree of dolomitisation. All the samples contain significant amount of C_{org} (in form of graphite) ranging from 0.1 to 1.0%, $0.25 \pm 0.13\%$ on average. The C_{org} content is positively correlated with SiO_2 content, $r=0.40$ (Fig. 19).

The dolomite marbles are characterised by the MgO/CaO ratios (Table 1, Fig. 19), which are very close to that of stoichiometric dolomite (21.9% MgO, 30.4% CaO).

10. CARBON, OXYGEN AND STRONTIUM ISOTOPES

The 46 samples out of 140 were selected for carbon, oxygen and strontium isotope analyses. Samples of calcite marbles having $Mn/Sr > 0.1$ were excluded from the isotope analyses. Table 2 summarises isotope analyses and the related data on trace and major element abundances. For the special purpose of chemostratigraphy and indirect age constraints by using carbon and strontium isotope calibration curves, it is essential to discriminate between altered and the least altered samples. In general, both metamorphism and non-fermentative diagenesis tends to deplete carbonates in Sr and enriched them in Mn (e.g., Brand & Veizer 1980). Hudson (1977) found that oxygen isotopes may be a sensitive indicator of diagenetic alteration. Diagenesis commonly decreases $\delta^{18}O$ and the effect of diagenesis can be revealed by $\delta^{13}C$ and $\delta^{18}O$ cross-plot. Oxygen isotopes are commonly much more easily affected by

Table 1. Chemical composition of carbonate rocks of the Beirn area.

Sample nn	Rock description	Litho-facies	SiO ₂	Al ₂ O ₃	Fe ₂ O ₃	TiO ₂	MgO _{tot}	CaO _{tot}	Na ₂ O	K ₂ O	MnO	P ₂ O ₅	C _{tot}	C _{org}	CaO _{as}	MgO _{as}
			%													
Pure calcite marbles																
97-66	Grey, banded, coarse-grained	1	0.40	0.06	0.11	0.01	0.21	54.69	-	0.02	0.00	0.12	12.6	0.12	54.71	0.24
97-64	Grey, banded, coarse-grained	1	0.70	0.17	0.19	0.02	0.17	54.35	-	0.05	0.01	0.13	12.5	0.12	54.57	0.24
96-58	Grey, banded, coarse-grained	1	1.46	0.41	0.20	0.02	0.23	54.12	-	0.10	0.01	0.08	12.6	0.10	54.03	0.10
97-45	Grey, banded, coarse-grained	2	1.58	0.43	0.37	0.03	0.26	53.67	-	0.07	0.01	0.11	12.4	0.13	53.60	0.40
96-60	Grey, banded, coarse-grained	1	1.94	0.54	0.12	0.03	0.37	53.48	0.38	0.14	0.01	0.09	12.2	0.17	53.46	0.34
97-67	Grey, banded, coarse-grained	1	2.13	0.32	0.16	0.02	0.22	53.46	-	0.10	0.01	0.10	12.1	0.18	53.31	0.26
96-65	Grey, banded, coarse-grained	1	2.34	0.68	0.20	0.04	0.29	53.30	-	0.16	0.01	0.08	12.3	0.17	53.18	0.26
97-65	Grey, banded, coarse-grained	1	1.85	0.60	0.26	0.03	0.25	53.54	-	0.16	0.01	0.10	12.2	-	53.03	0.18
97-32	Grey, banded, coarse-grained	1	2.17	0.77	0.45	0.05	0.28	52.77	-	0.22	0.01	0.10	12.0	0.17	52.81	0.30
97-34	Grey, banded, coarse-grained	1	2.67	0.72	0.28	0.04	0.31	52.76	0.17	0.11	0.01	0.11	12.0	0.18	52.72	0.38
EX29	Pale gray, banded	1	2.63	0.75	0.25	0.03	0.26	52.40	-	0.16	0.01	0.09	12.8	n.d.	n.d.	n.d.
Relatively pure calcite marbles																
EX30	White, massive	*	4.37	1.05	0.28	0.05	0.32	52.35	0.33	0.24	0.01	0.10	12.4	n.d.	n.d.	n.d.
97-35	Grey, banded, coarse-grained	1	3.17	0.78	0.33	0.04	0.33	52.34	0.23	0.11	0.02	0.09	12.0	0.27	52.31	0.34
96-59	Grey, banded, coarse-grained	1	3.70	0.82	0.27	0.04	0.33	52.33	-	0.24	0.01	0.06	11.9	0.15	52.10	0.36

Table 1. (continued).

Sample nn	Rock description	Litho-facies	SiO ₂	Al ₂ O ₃	Fe ₂ O ₃	TiO ₂	MgO _{tot}	CaO _{tot}	Na ₂ O	K ₂ O	MnO	P ₂ O ₅	C _{tot}	C _{org}	CaO _{as}	MgO _{as}
			%													
Relatively pure calcite marbles																
96-1	Grey, banded, fine-grained	4	4.07	0.73	0.30	0.04	0.64	52.07	0.13	0.14	0.01	0.13	12.0	0.13	52.05	0.62
97-51	Grey, banded, coarse-grained	1	3.73	1.15	0.41	0.06	0.31	52.09	0.12	0.21	0.02	0.12	12.1	0.23	51.97	0.20
96-50	Grey, banded, fine-grained	1	4.03	0.91	0.31	0.04	0.31	52.03	0.12	0.16	0.01	0.09	12.8	0.21	51.78	0.33
96-23	Grey, banded, fine-grained	2	4.72	1.02	0.28	0.06	0.42	51.66	0.17	0.18	0.01	0.07	13.5	0.11	51.62	0.46
96-38	Grey, banded, coarse-grained	3	4.63	1.07	0.39	0.05	0.45	51.58	0.26	0.27	0.01	0.08	11.9	0.23	51.42	0.24
Impure calcite marbles																
96-46	Grey, banded, fine-grained	*	4.36	1.09	0.36	0.06	0.41	52.00	-	0.21	0.01	0.09	13.4	0.28	51.40	0.36
EX28	Pale gray marble	2	5.38	1.17	0.42	0.06	0.34	51.48	0.21	0.21	0.01	0.12	12.4	n.d.	n.d.	n.d.
97-49	Grey, banded, coarse-grained	1	4.07	1.32	1.06	0.06	0.34	51.07	0.56	0.04	0.07	0.11	12.0	0.13	50.89	0.42
96-2	Grey, banded, fine-grained	3	4.96	1.03	0.52	0.05	0.59	50.50	0.13	0.26	0.01	0.08	12.0	0.24	50.88	0.58
97-46	Grey, banded, coarse-grained	2	4.77	1.41	0.60	0.07	0.30	50.89	-	0.31	0.01	0.08	11.8	0.19	50.86	0.34
97-63	Grey, banded, coarse-grained	1	5.43	1.37	0.43	0.08	0.28	50.81	-	0.41	0.01	0.09	11.7	0.19	50.85	0.26
96-21	Grey, banded, fine-grained	2	4.85	1.47	0.48	0.08	0.49	50.34	0.65	0.36	0.01	0.07	11.7	0.19	50.74	0.50
96-15	White, massive, coarse-grained	1	6.27	0.26	0.83	0.02	0.67	50.10	-	0.06	0.03	0.05	11.8	-	50.47	0.61
96-56	Grey, banded, coarse-grained	1	6.03	1.43	0.42	0.07	0.41	50.49	0.19	0.31	0.01	0.06	11.6	0.18	50.31	0.28
97-31	Grey, banded, coarse-grained	2	6.07	1.63	0.61	0.08	0.30	50.23	0.38	0.12	0.02	0.08	11.3	0.20	50.27	0.18

Table 1. (continued).

Sample nn	Rock description	Litho-facies	SiO ₂	Al ₂ O ₃	Fe ₂ O ₃	TiO ₂	MgO _{tot}	CaO _{tot}	Na ₂ O	K ₂ O	MnO	P ₂ O ₅	C _{tot}	C _{org}	CaO _{as}	MgO _{as}
			%													
Impure calcite marbles																
97-47	Grey, banded, coarse-grained	2	5.61	1.90	0.73	0.09	0.32	50.24	-	0.40	0.01	0.08	11.7	0.16	50.23	0.18
96-62	Grey, banded, coarse-grained	1	5.73	1.66	0.64	0.09	0.48	50.20	0.31	0.30	0.01	0.06	11.6	0.21	50.20	0.40
97-26	Grey, banded, coarse-grained	2	5.42	1.67	0.48	0.08	0.28	50.68	-	0.29	0.02	0.10	11.7	0.21	50.07	0.34
96-57	Grey, banded, coarse-grained	2	6.60	0.92	0.21	0.05	0.35	50.53	0.23	0.08	0.01	0.06	11.7	0.21	49.84	0.34
96-22	Grey, banded, coarse-grained	2	6.29	1.65	0.64	0.07	0.54	49.68	0.45	0.20	0.01	0.07	11.6	0.20	49.71	0.46
96-44	Grey, banded, coarse-grained	*	6.91	1.65	0.60	0.08	0.60	49.45	0.18	0.36	0.01	0.07	11.6	0.19	49.43	0.56
96-55	Grey, banded, coarse-grained	1	7.02	1.78	0.29	0.04	0.32	49.93	0.30	0.23	0.01	0.09	11.4	0.21	49.23	0.18
97-68	Grey, banded, coarse-grained	1	6.28	1.69	0.56	0.07	1.00	49.58	0.45	0.19	0.01	0.07	11.5	0.22	48.94	0.62
96-20	Grey, banded, coarse-grained	2	7.42	2.37	0.54	0.11	0.49	48.97	0.20	0.43	0.01	0.06	11.4	0.16	48.60	0.50
96-63	Grey, banded, coarse-grained	1	8.02	1.95	0.43	0.09	0.48	49.05	0.49	0.40	0.01	0.07	11.1	0.13	48.51	0.44
96-14	Grey, banded, fine-grained	2	7.25	2.21	0.57	0.12	0.67	49.38	0.17	0.22	0.02	0.08	11.4	0.18	48.43	0.56
96-17	Grey, banded, coarse-grained	1	7.56	2.09	0.66	0.08	0.71	49.05	0.21	0.42	0.01	0.06	11.5	0.21	48.28	0.68
97-69	Grey, banded, coarse-grained	2	7.94	1.51	0.70	0.06	1.71	49.07	0.37	0.14	0.01	0.08	11.0	0.16	48.17	0.71
96-51	Grey, banded, coarse-grained	2	8.52	2.30	0.73	0.09	0.41	47.98	0.67	0.35	0.02	0.10	11.2	0.41	47.94	0.36
96-52	Grey, banded, coarse-grained	2	8.32	2.26	0.67	0.10	0.48	48.33	0.19	0.49	0.01	0.10	11.2	0.31	47.75	0.48

Table 1. (continued).

Sample nn	Rock description	Litho-facies	SiO ₂	Al ₂ O ₃	Fe ₂ O ₃	TiO ₂	MgO _{tot}	CaO _{tot}	Na ₂ O	K ₂ O	MnO	P ₂ O ₅	C _{tot}	C _{org}	CaO _{as}	MgO _{as}
			%													
Impure calcite marbles																
97-60	Grey, banded, coarse-grained	2	8.33	2.83	1.24	0.13	0.46	47.84	0.19	0.68	0.03	0.08	11.1	0.24	47.61	0.50
97-48	Grey, banded, coarse-grained	1	8.43	2.43	1.11	0.11	0.39	47.96	1.10	0.05	0.07	0.07	11.3	0.18	47.56	0.38
96-64	Grey, banded, coarse-grained	1	9.12	2.32	0.54	0.09	0.58	48.26	0.61	0.37	0.02	0.07	10.9	-	47.47	0.44
96-42	Grey, banded, coarse-grained	*	8.57	2.13	0.64	0.08	0.81	48.28	0.22	0.44	0.01	0.06	11.4	0.23	47.04	0.85
96-53	Grey, banded, coarse-grained	2	8.37	2.82	0.94	0.11	0.73	48.17	0.29	0.45	0.02	0.07	11.0	0.29	46.78	0.70
96-24	Grey, banded, coarse-grained	2	8.70	3.26	1.02	0.14	0.78	47.97	0.61	0.13	0.07	0.05	10.7	-	46.32	0.79
Very impure calcite marbles																
97-54	Grey, banded, coarse-grained	1	10.45	3.41	1.00	0.17	0.70	46.53	-	0.62	0.02	0.10	10.7	0.31	45.94	0.75
97-30	Grey, banded, coarse-grained	1	9.10	3.24	1.06	0.13	0.56	47.62	0.25	0.43	0.02	0.08	10.8	0.43	45.89	0.56
97-50	Grey, banded, coarse-grained	1	11.04	3.32	1.08	0.14	0.44	46.07	0.23	0.69	0.02	0.07	10.7	0.23	45.48	0.50
97-57	Grey, banded, coarse-grained	2	11.10	2.93	1.35	0.15	0.99	46.10	0.87	0.27	0.03	0.05	10.6	0.24	45.27	0.73
97-29	Grey, banded, coarse-grained	1	10.69	2.92	1.37	0.15	0.53	46.53	1.20	0.03	0.03	0.09	10.6	0.16	45.11	0.48
97-55	Grey, banded, coarse-grained	?	12.11	3.91	1.45	0.20	0.69	44.85	0.11	0.70	0.03	0.11	10.5	0.33	44.79	0.71
97-58	Grey, banded, coarse-grained	2	13.43	3.09	1.00	0.14	0.73	45.22	0.25	0.67	0.01	0.06	10.3	0.14	44.74	0.54
96-18	Grey, banded, coarse-grained	2	10.90	2.96	0.95	0.12	1.36	46.62	0.30	0.72	0.01	0.06	10.7	0.21	44.65	0.56
96-61	Grey, banded, coarse-grained	2	12.39	3.74	0.95	0.18	0.92	44.99	1.25	0.22	0.02	0.05	10.2	0.21	44.24	0.50

Table 1. (continued).

Sample nn	Rock description	Litho-facies	SiO ₂	Al ₂ O ₃	Fe ₂ O ₃	TiO ₂	MgO _{tot}	CaO _{tot}	Na ₂ O	K ₂ O	MnO	P ₂ O ₅	C _{tot}	C _{org}	CaO _{as}	MgO _{as}
			%													
Very impure calcite marbles																
97-33	Grey, banded, coarse-grained	1	11.30	3.77	1.38	0.18	0.48	44.93	0.23	0.88	0.02	0.05	9.9	-	44.04	0.48
96-37	Grey, banded, coarse-grained	3	12.54	3.20	1.06	0.14	1.05	44.94	0.36	0.73	0.01	0.05	10.3	0.25	43.88	0.95
97-62	Grey, banded, coarse-grained	2	13.31	3.73	1.29	0.16	0.64	44.64	0.46	0.79	0.02	0.06	10.2	0.13	43.87	0.36
96-19	Grey, banded, coarse-grained	?	13.46	3.99	1.27	0.18	0.82	43.98	0.48	0.87	0.02	0.03	10.3	0.38	42.98	0.77
96-39	Grey, banded, coarse-grained	3	13.70	3.65	1.25	0.15	1.04	43.71	0.44	0.70	0.02	0.06	9.8	0.18	42.19	0.67
96-29	Grey, banded, coarse-grained	2	14.67	4.50	1.12	0.20	0.78	43.75	1.53	0.13	0.04	0.04	10.0	0.19	41.97	0.75
97-24	Grey, banded, coarse-grained	2	16.25	3.95	1.21	0.21	0.47	43.05	0.34	0.74	0.01	0.09	9.9	0.46	41.89	0.14
97-52	Grey, banded, coarse-grained	3	16.11	4.89	1.28	0.22	0.56	42.26	0.25	0.82	0.02	0.06	9.9	0.43	41.35	0.60
96-26	Grey, banded, coarse-grained	2	15.37	4.46	1.04	0.22	0.97	42.69	1.62	0.25	0.03	0.02	10.1	0.25	41.29	0.97
96-30	Grey, banded, coarse-grained	2	17.78	2.95	1.66	0.15	1.12	42.65	0.32	0.57	0.03	0.04	9.6	0.25	41.29	0.87
97-28	Grey, banded, coarse-grained	3	13.19	3.78	3.02	0.46	1.30	42.39	0.48	0.14	0.12	0.09	9.6	0.13	40.27	0.56
97-53	Grey, banded, coarse-grained	1	0.70	0.17	0.17	0.02	0.16	54.46	-	0.04	0.00	0.10	9.5	0.43	39.79	0.18
96-41	Grey, banded, coarse-grained	*	16.72	4.85	1.58	0.23	1.00	42.22	0.23	0.63	0.02	0.19	10.0	1.04	39.48	0.83
97-27	Grey, banded, coarse-grained	2	18.02	4.98	1.53	0.25	0.53	40.35	0.41	1.03	0.02	0.05	9.4	0.45	38.97	0.40
96-16	Grey, banded, coarse-grained	1	18.22	4.36	1.28	0.19	0.98	39.72	0.62	0.82	0.01	0.03	9.4	0.29	38.81	0.76
97-43	Grey, banded, coarse-grained	2	18.39	4.73	1.72	0.24	1.02	41.28	1.51	0.38	0.03	0.03	9.0	0.27	38.24	0.71
96-25	Grey, banded, coarse-grained	2	18.94	5.69	1.86	0.26	1.31	39.95	0.72	1.08	0.02	0.01	11.4	0.23	37.61	0.91

Table 1. (continued.)

Sample nn	Rock description	Litho-facies	SiO ₂	Al ₂ O ₃	Fe ₂ O ₃	TiO ₂	MgO _{tot}	CaO _{tot}	Na ₂ O	K ₂ O	MnO	P ₂ O ₅	C _{tot}	C _{org}	CaO _{as}	MgO _{as}
			%													
Very impure calcite marbles																
97-25	Grey, banded, coarse-grained	2	20.42	5.96	1.65	0.28	0.71	39.17	0.58	1.02	0.03	0.04	8.9	0.47	37.19	0.26
96-48	Grey, banded, coarse-grained	2*	21.44	4.75	1.14	0.19	1.62	39.91	0.39	1.35	0.01	0.03	8.7	0.27	36.37	0.30
96-43	Grey, banded, coarse-grained	*	22.20	6.23	1.38	0.23	0.88	38.75	0.74	0.91	0.03	0.06	9.1	0.29	36.19	0.83
97-41	Grey, banded, coarse-grained	2	21.70	7.24	1.22	0.30	0.85	36.25	1.55	1.32	0.02	-	8.5	0.25	35.26	0.69
96-4	Grey, banded, fine-grained	4*	20.79	5.34	1.83	0.27	2.45	39.92	0.50	0.97	0.02	0.04	8.1	-	34.97	0.47
96-45	Grey, banded, coarse-grained	*	19.99	6.49	2.10	0.29	1.01	37.01	0.72	1.09	0.04	0.03	8.3	0.55	34.16	0.38
97-44	Grey, banded, coarse-grained	2	23.98	7.10	2.11	0.36	1.17	36.04	0.58	1.33	0.02	-	7.9	0.29	33.89	0.83
96-54	Grey, banded, coarse-grained	2	25.37	6.11	1.82	0.28	0.88	37.01	0.48	1.25	0.03	-	8.1	0.19	33.65	0.52
96-12	Grey, banded, fine-grained	2	24.86	4.99	1.66	0.23	1.65	36.16	0.58	0.79	0.03	0.10	7.6	0.15	33.57	0.53
97-61	Grey, banded, coarse-grained	2	23.90	7.41	2.41	0.30	0.81	37.31	0.49	0.91	0.03	-	7.6	0.12	32.70	0.44
96-32	Grey, banded, coarse-grained	2	28.95	7.01	2.69	0.35	1.19	32.52	0.77	1.48	0.04	0.01	7.1	-	29.39	0.56
96-35	Grey, banded, coarse-grained	2	34.72	9.07	3.48	0.48	1.50	29.35	0.80	1.84	0.04	0.01	5.6	0.52	22.73	0.24
96-34	Grey, banded, coarse-grained	2	39.30	8.12	2.92	0.45	1.64	24.68	0.85	1.65	0.04	-	5.2	0.39	20.83	0.99
96-49	Grey, banded, coarse-grained	2*	38.25	10.31	3.84	0.47	2.68	25.92	1.03	2.14	0.02	-	7.6	0.30	18.49	0.32
97-38	Grey, banded, coarse-grained	2	41.54	8.96	4.39	0.50	1.92	25.37	0.47	1.75	0.04	-	4.2	0.35	17.02	0.56
97-39	Grey, banded, coarse-grained	2	40.50	8.43	3.00	0.46	2.97	23.02	0.83	1.30	0.02	-	3.9	0.31	15.78	0.69
96-9	Grey, banded, coarse-grained	2	48.17	11.16	3.52	0.51	2.74	23.83	0.54	1.95	0.06	0.29	1.9	0.40	8.09	0.36

Table 1. (continued).

Sample nn	Rock description	Litho-facies	SiO ₂	Al ₂ O ₃	Fe ₂ O ₃	TiO ₂	MgO _{tot}	CaO _{tot}	Na ₂ O	K ₂ O	MnO	P ₂ O ₅	C _{tot}	C _{org}	CaO _{as}	MgO _{as}
			%													
Dolomitised calcite marbles																
96-13	Grey, banded, fine-grained	2	4.31	0.44	1.02	0.03	5.60	45.99	0.20	0.10	0.03	0.03	11.7	-	45.93	3.66
97-56	Grey, banded, coarse-grained	2	5.10	1.47	0.73	0.07	1.84	49.49	0.74	0.03	0.02	0.08	11.8	0.15	49.57	1.95
96-6	Grey, banded, fine-grained	4*	19.59	4.72	1.43	0.27	2.41	40.36	0.34	1.09	0.01	0.04	9.1	0.62	36.37	1.55
97-40	Grey, banded, coarse-grained	?	5.98	0.47	0.35	0.03	1.71	50.38	-	0.03	0.01	0.07	11.7	0.13	49.40	1.27
96-28	Grey, banded, coarse-grained	2	16.17	4.22	1.35	0.20	1.25	42.67	0.64	0.90	0.02	0.03	9.6	0.21	40.79	1.27
96-36	Grey, banded, coarse-grained	3	29.29	4.86	1.85	0.22	2.43	34.74	0.62	0.86	0.04	-	7.2	0.20	30.48	1.26
97-42	Grey, banded, coarse-grained	2	25.05	6.75	1.04	0.08	1.59	34.99	2.25	1.48	0.04	-	7.8	-	33.20	1.17
96-5	Grey, banded, fine-grained	4*	13.75	2.68	0.96	0.14	1.40	44.54	0.22	0.78	0.01	0.05	10.5	0.43	43.26	1.14
96-27	Grey, banded, coarse-grained	2	19.03	5.40	1.45	0.27	1.11	37.96	0.58	1.28	0.02	-	8.9	0.22	37.95	1.09
97-37	Grey, banded, coarse-grained	2 or 4	44.44	10.68	3.61	0.58	1.92	22.05	0.88	2.05	0.03	-	3.2	-	13.76	1.03
96-31	Grey, banded, coarse-grained	2	12.46	3.51	2.23	0.19	1.24	44.56	0.40	0.85	0.04	0.05	10.1	0.29	43.20	1.07
96-47	Grey, banded, coarse-grained	*	10.13	2.72	1.01	0.12	0.95	45.59	0.29	0.55	0.01	0.06	11.7	-	45.58	1.01
96-33	Grey, banded, coarse-grained	2	36.05	7.61	2.86	0.38	1.34	27.84	0.71	1.56	0.04	-	5.8	0.29	24.98	1.02
Relatively pure dolomite marbles																
96-7	White, massive, coarse-grained	5	1.06	0.04	0.10	-	23.57	30.49	-	0.01	0.00	0.07	13.3	-	n.d.	n.d.
96-10	White, massive, coarse-grained	5	2.13	0.19	0.14	0.01	23.19	30.76	-	0.05	0.01	0.05	12.6	-	n.d.	n.d.

Table 1. (continued).

Sample nn	Rock description	Litho-facies	SiO ₂	Al ₂ O ₃	Fe ₂ O ₃	TiO ₂	MgO _{tot}	CaO _{tot}	Na ₂ O	K ₂ O	MnO	P ₂ O ₅	C _{tot}	C _{org}	CaO _{as}	MgO _{as}
			%													
Relatively pure dolomite marbles																
96-11	Grey, banded, coarse-grained	5	4.79	0.12	0.37	-	22.90	29.95	-	0.02	0.03	0.05	12.4	-	n.d.	n.d.
EX27	White, massive, coarse-grained	5	0.18	0.02	0.05	-	22.82	31.08	0.51	0.02	-	0.05	14.3	n.d.	n.d.	n.d.
96-8	White, massive, coarse-grained	5	0.36	0.20	0.57	0.01	21.35	30.16	0.12	0.05	0.02	0.37	13.7	0.46	n.d.	n.d.
Impure dolomite marbles																
96-3	Grey, coarse-grained	5	22.95	1.41	1.42	0.04	18.63	25.95	0.28	0.31	0.03	0.04	6.5	0.17	n.d.	n.d.
96-40	White, massive, coarse-grained	5	20.01	-	0.09	-	22.17	28.19	-	-	0.00	0.14	7.8	-	n.d.	n.d.

'Dashes'-below detection limits: 0.1% for Al₂O₃, Na₂O and C_{org}; 0.01% for TiO₂, MnO, P₂O₅.

'n.d.' - not determined.

'*' - Sample location is outside of the mapped area.

'?' - Lithofacial belonging is unclear.

Table 2. Chemical and isotope composition of carbonate rocks from the Beirn area.

Sample nn	IS	Mn	Rb	Sr ⁺	Sr ^v	Mg/Ca	Mn/Sr	δ ¹³ C	δ ¹⁸ O	⁸⁷ Rb/ ⁸⁶ Sr	⁸⁷ Sr/ ⁸⁶ Sr measured	⁸⁷ Sr/ ⁸⁶ Sr initial	Minerals in IS
								ppm					

Lithofacies 1, calcite marble

96-55	6.8	62	17.6	2031	1961	0.005	0.03	5.6	17.3	0.0263	0.70665	0.70642	Qu, Fsp, Ms
96-57	7.7	100	0.009	2264	2485	0.006	0.04	5.2	19.4	0.0001	0.70677	0.70676	Ms, Qu, Fsp
96-58	2.3	46	0.21	2090	2074	0.004	0.02	5.3	22.9	0.0001	0.70655	0.70655	Ms, Qu, Fsp
96-59	3.9	54	0.02	2046	2039	0.005	0.03	5.6	21.7	0.0001	0.70667	0.70667	Ms, Qu, Fsp
96-60	2.5	39	0.05	2163	2132	0.006	0.02	5.4	21.3	0.0001	0.70657	0.70657	Ms, Qu, Fsp
96-65	3.2	39	0.06	2313	2309	0.005	0.02	5.2	22.8	0.0001	0.70665	0.70665	Ms, Qu
97-30	15.1	154	8.75	2079	1990	0.010	0.07	2.9	18.8	0.0129	0.70697	0.70686	Qu, Fsp, Am
97-32	3.7	77	0.191	2013	2136	0.004	0.04	4.0	19.5	0.0003	0.70708	0.70707	Ms, Qu
97-33	17.8	154	11.4	1912	1865	0.009	0.08	4.0	15.2	0.0179	0.70724	0.70708	Ms, Chl, Qu, Fsp
97-35	3.6	154	0.193	1863	1741	0.005	0.08	n.d.	n.d.	0.0003	0.70687	0.70687	Qu, Fsp, Ms
97-50	15.7	154	3.75	1860	1893	0.008	0.08	5.5	19.8	0.0058	0.70704	0.70699	Ms, Qu, Fsp
97-51	4.2	154	0.161	1976	2010	0.005	0.08	5.7	23.4	0.0002	0.70665	0.70664	Qu, Ms, Fsp
97-52	22.8	154	11.9	1790	1460	0.011	0.09	4.1	24.8	0.0239	0.70707	0.70686	Ms, Qu, Fsp
97-53	26.7	0	14.4	1348	1378	0.002	0.00	3.4	23.7	0.0306	0.70743	0.70716	Ms, Qu, Fsp
97-67	1.1	77	0.039	1947	1987	0.003	0.04	4.5	21.2	0.0001	0.70665	0.70665	Qu
97-68	9.2	77	4.20	1941	1886	0.017	0.04	4.7	16.4	0.0065	0.70673	0.70667	Qu, Ms, Am
EX29	3.7	46	0.141	2112	2119	0.004	0.02	4.9	16.5	0.0002	0.70656	0.70656	Ms, Qu, Fsp

Table 2. (continued).

Sample nn	IS	Mn	Rb	Sr ⁺	Sr ^v	Mg/Ca	Mn/Sr	δ ¹³ C	δ ¹⁸ O	⁸⁷ Rb/ ⁸⁶ Sr	⁸⁷ Sr/ ⁸⁶ Sr measured	⁸⁷ Sr/ ⁸⁶ Sr initial	Minerals in IS
								ppm					

Lithofacies 1, calcite marble

EX30* 3.9 54 0.506 1967 1971 0.005 0.03 5.7 19.4 0.0008 0.70676 0.70675 Ms, Qu, Fsp

Lithofacies 2, calcite marble

96-17 10.1 62 1.83 2303 2336 0.012 0.03 n.d. n.d. 0.0003 0.70715 0.70713 Ms, Qu, Fsp
 96-21 6.2 85 0.162 2131 2184 0.008 0.04 8.1 19.8 0.0002 0.70691 0.70691 Ms, Qu, Fsp
 96-23 4.7 77 0.127 2112 2138 0.007 0.04 7.5 19.9 0.0002 0.70695 0.70695 Ms, Qu, Fsp
 96-50 4.8 85 0.15 2339 2409 0.005 0.04 8.0 20.4 0.0002 0.70705 0.70705 Ms, Qu, Fsp
 96-52 10.4 92 1.63 1938 2024 0.008 0.05 7.2 17.4 0.0024 0.70704 0.70702 Ms, Qu, Fsp
 97-24 22.4 77 3.87 1643 1744 0.009 0.05 6.5 20.5 0.0065 0.70725 0.70720 Qu, Fsp, Ms
 97-26 7.6 154 2.45 2229 2254 0.005 0.07 6.8 22.8 0.0032 0.70703 0.70700 Qu, Fsp, Ms
 97-27 23.9 154 10.9 1832 2086 0.011 0.08 6.4 21.6 0.0154 0.70746 0.70732 Qu, Fsp, Ms
 97-31 8.1 154 0.214 2091 2517 0.005 0.07 6.8 19.8 0.0002 0.70695 0.70695 Ms, Qu, Fsp
 97-34 4.8 77 0.222 1959 2063 0.005 0.04 4.5 20.9 0.0003 0.70981 0.70981 Ms, Qu, Fsp
 97-40 7.3 77 0.212 1766 1919 0.029 0.04 1.3 17.9 0.0003 0.71000 0.70999 Ms, Chl, Am, Qu
 97-41 31.1 154 19.7 1839 1894 0.020 0.08 4.2 16.9 0.0305 0.70761 0.70734 Ms, Chl, Qu, Fsp
 97-45 2.6 77 0.192 1942 2056 0.004 0.04 7.4 21.9 0.0003 0.70683 0.70683 Qs, Ms, Fsp
 97-46 4.9 77 0.209 2104 2035 0.005 0.04 7.1 20.3 0.0003 0.70703 0.70703 Ms, Qu, Fsp

Table 2. (continued).

Sample nn	IS	Mn	Rb	Sr ⁺	Sr ^v	Mg/Ca	Mn/Sr	δ ¹³ C	δ ¹⁸ O	⁸⁷ Rb/ ⁸⁶ Sr	⁸⁷ Sr/ ⁸⁶ Sr measured	⁸⁷ Sr/ ⁸⁶ Sr initial	Minerals in IS
								ppm					

Lithofacies 2, calcite marble

97-47	7.2	77	0.647	2050	2131	0.005	0.04	7.2	19.6	0.0009	0.70693	0.70693	Ms, Qu, Fsp
97-56	6.8	154	0.295	1644	1719	0.031	0.09	4.0	14.1	0.0005	0.70739	0.70738	Ms, Fsp, Sil
97-58	16.6	77	10.9	1771	1894	0.014	0.04	5.7	21.2	0.0168	0.70741	0.70727	Ms, Qu, Fsp, Sil
EX28	6.8	85	1.10	1916	2093	0.006	0.04	7.1	17.4	0.0016	0.70693	0.70691	Qu, Ms, Fsp

Lithofacies 3, calcite marble

96-37	16.6	108	13.1	2030	2014	0.020	0.05	8.3	20.2	0.0190	0.70741	0.70724	Ms, Qu, Fsp, Am
96-38	5.5	54	0.209	2453	2556	0.007	0.02	8.1	22.9	0.0002	0.70733	0.70732	Ms, Qu, Fsp
96-42*	12.2	85	2.89	2364	2372	0.014	0.04	8.1	21.7	0.0036	0.70725	0.70722	Ms, Qu, Fsp
96-44*	8.5	69	0.28	2385	2475	0.010	0.03	8.4	21.9	0.0004	0.70727	0.70727	Ms, Qu, Fsp

Lithofacies 4, calcite marble

96-1	4.4	69	0.105	1795	1829	0.010	0.04	5.9	21.1	0.0002	0.70751	0.70750	Ms, Qu, Fsp
96-2	3.8	54	0.217	1978	2029	0.010	0.03	4.6	18.2	0.0003	0.70749	0.70749	Ms, Qu

Lithofacies 5, dolomite marble

96-7	1.6	23	1.70	88	79.3	0.653	0.26	7.8	27.5	0.0631	0.70725	0.70670	Am, Sp
------	-----	----	------	----	------	-------	------	-----	------	--------	---------	---------	--------

Table 2. (continued).

Sample nn	IS	Mn	Rb	Sr*	Sr ^v	Mg/Ca	Mn/Sr	δ ¹³ C	δ ¹⁸ O	⁸⁷ Rb/ ⁸⁶ Sr	⁸⁷ Sr/ ⁸⁶ Sr measured	⁸⁷ Sr/ ⁸⁶ Sr initial	Minerals in IS
								ppm					

Lithofacies 5, dolomite marble

<i>96-11</i>	8.3	193	2.50	97	94.7	0.646	1.98	7.2	24.2	0.0776	0.70802	0.70735	Am, Sp
<i>96-40</i>	27.0	15	0.15	56	73.3	0.665	0.28	1.3	18.2	0.0113	0.70766	0.70756	Di, Sp
<i>EX27</i>	0.5	2	0.04	77	72.8	0.620	0.03	7.6	23.7	0.0021	0.70721	0.70719	Qu, Ms

IS – insoluble residue.

'n.d.' - not determined.

Sr* - Total Sr analysed by XRF.

Sr^v - Acid soluble Sr analysed by standard isotope dilution and solid-source mass spectrometry.

The initial ⁸⁷Sr/⁸⁶Sr ratios are calculated under the assumption that the age of these rocks is equal to 610 Ma.

Bold-face letter - the 'least altered' samples (see discussion in text).

Italic-face letter - altered samples.

'*' - Samples located outside of the mapped area.

Abbreviation used: Am – amphibole, Chl – chlorite, Di – diopside, Fsp – feldspar, Ms – muscovite, Qu – quartz, Sp – serpentine.

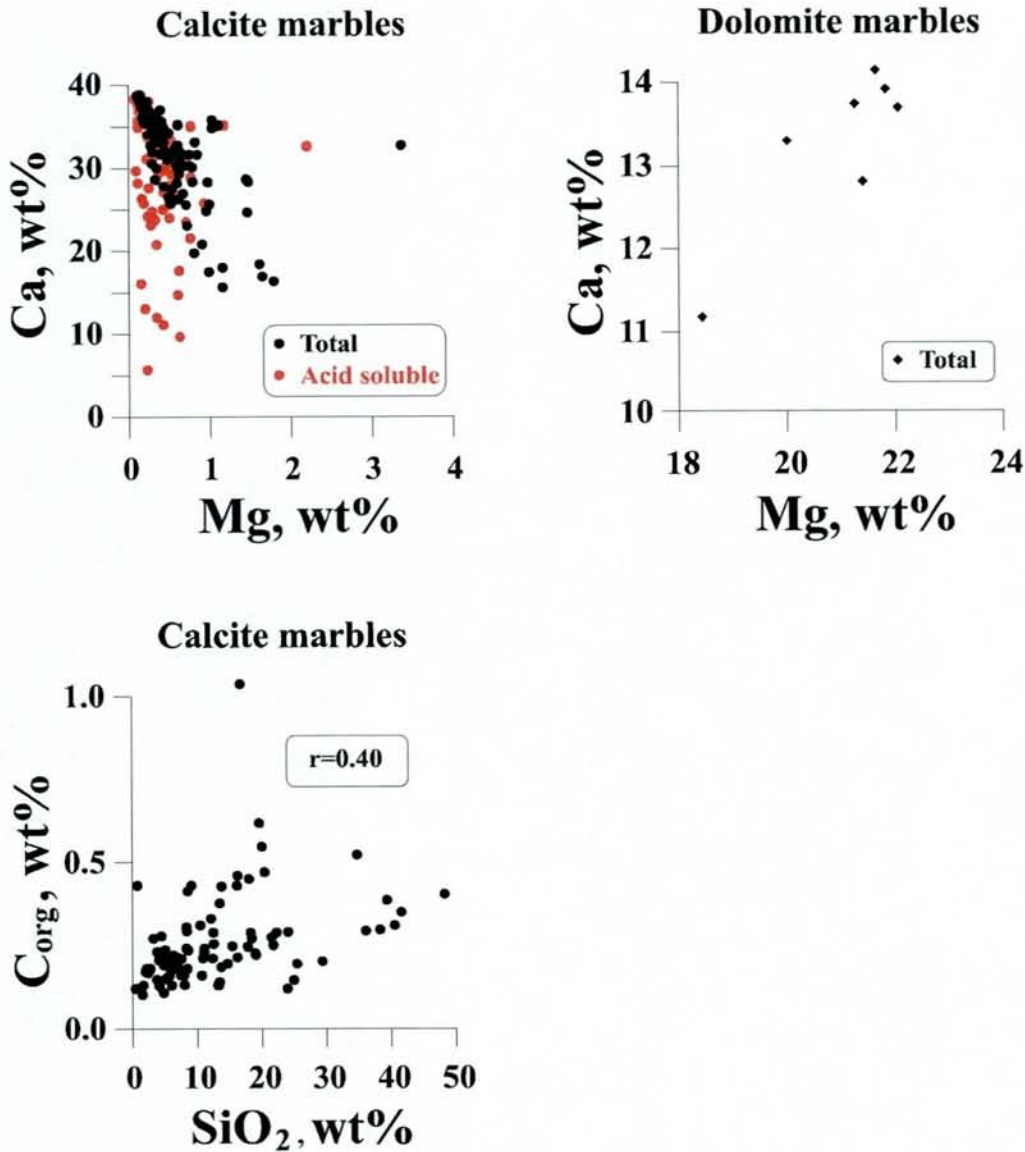


Figure 19. Ca, Mg, SiO₂, C_{org} cross-plots for the Sokumfjell marbles.

exchangeable oxygen derived from either meteoric water or interstitial fluids at elevated temperatures (e.g. Fairchild et al. 1990) whereas $\delta^{13}\text{C}$ may be buffered by pre-existing carbonate. In general, depletion in both oxygen and carbon isotope values may be considerable during late diagenesis as well as in the course of low-grade metamorphism accompanied by deformation (Guerrera et al. 1997).

Carbon and oxygen isotope values versus Mn/Sr ratios demonstrate that calcite marbles of all lithofacies were affected by alteration though to a different extent and in a different manner

(Fig. 20). Lithofacies 1 and 3 shows no covariation between $\delta^{18}\text{O}$ and $\delta^{13}\text{C}$ whereas Lithofacies 2 and 4 are characterised by strong positive correlation (Fig. 20a). This suggests

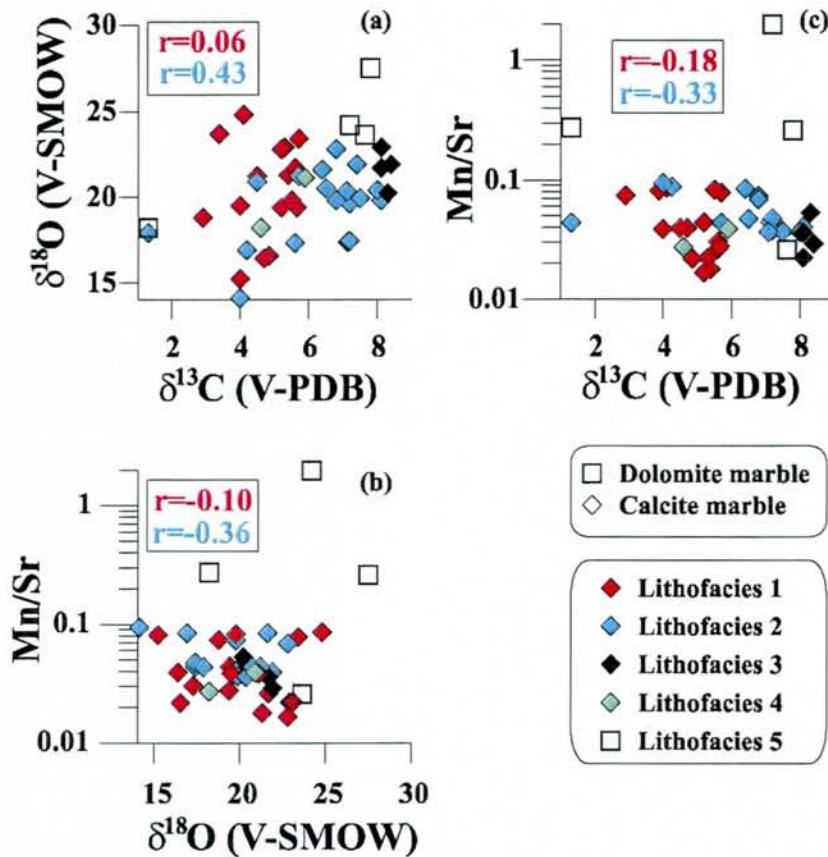


Figure 20. $\delta^{13}\text{C}$, $\delta^{18}\text{O}$, Mn/Sr cross-plots for the Sokumfjell marbles.

less alteration in the first group in particular with respect to $\delta^{13}\text{C}$. As far as Lithofacies 1 and 2 are concerned this statement is in agreement with more significant negative correlation between Mn/Sr ratios and both carbon and oxygen isotopes measured from Lithofacies 2 (Figs. 20b, c). The Mn/Sr ratios, carbon and oxygen isotopes plotted against Mg/Ca ratios (Fig. 21) confirm this observation and indicate that $\delta^{18}\text{O}$ and $\delta^{13}\text{C}$ resetting was likely linked to dolomitisation. Although Fig. 21 demonstrates that all lithofacies were affected by alterations, again, Lithofacies 1 exhibit less significant dependence of $\delta^{18}\text{O}$ and $\delta^{13}\text{C}$ from Mg/Ca ratios. However, in all lithofacies Mg/Ca-Mn/Sr covariance is very strong as defined by $r=0.45$, 0.50 and 0.99 for Lithofacies 1, 2 and 3, respectively.

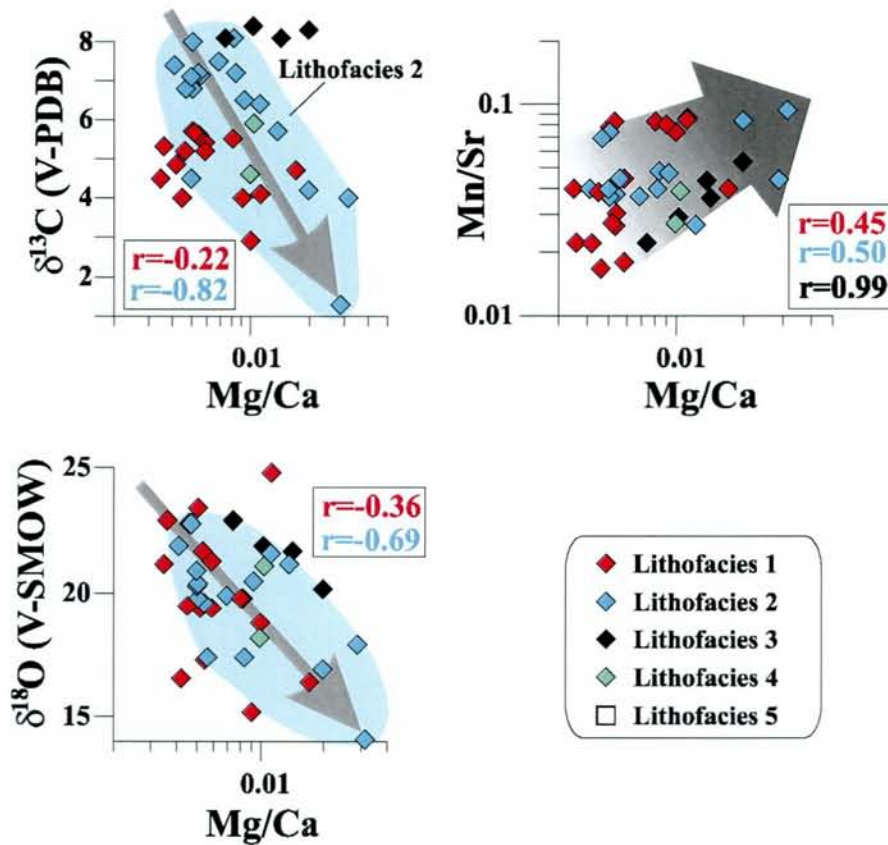


Figure 21. Oxygen and carbon isotopes versus Mg/Ca ratios for the Sokumfjell marbles. Arrows indicate alteration trends caused by dolomitisation.

From the 42 samples of calcite marbles analysed for carbon and oxygen isotopes, 34 show very low Mn/Sr values (≤ 0.07) and high Sr concentration (2104 ± 240 ppm), and 8 samples have Mn/Sr ranging from >0.07 to 0.09 and Sr 1833 ± 194 ppm: This suggests that the first group is better preserved whereas the second may include altered samples in terms of trace element chemistry. The dolomite marbles have Sr and Mn/Sr average values of 80 ppm and 0.64, respectively. Thus, the second group of calcite marbles and all dolomite samples are excluded from further discussion.

A plot of $^{87}\text{Sr}/^{86}\text{Sr}$ versus $1/\text{Sr} \times 1000$ (Fig. 22a) suggests that two measurements (Lithofacies 2, sample 97-34, 0.70981; sample 97-40, 0.70999) definitely have postdepositional enrichment in ^{87}Sr , and therefore should also be excluded from further consideration. For the remaining samples of Lithofacies 1 and 2, the $^{87}\text{Sr}/^{86}\text{Sr}$ values still appears to be dependent

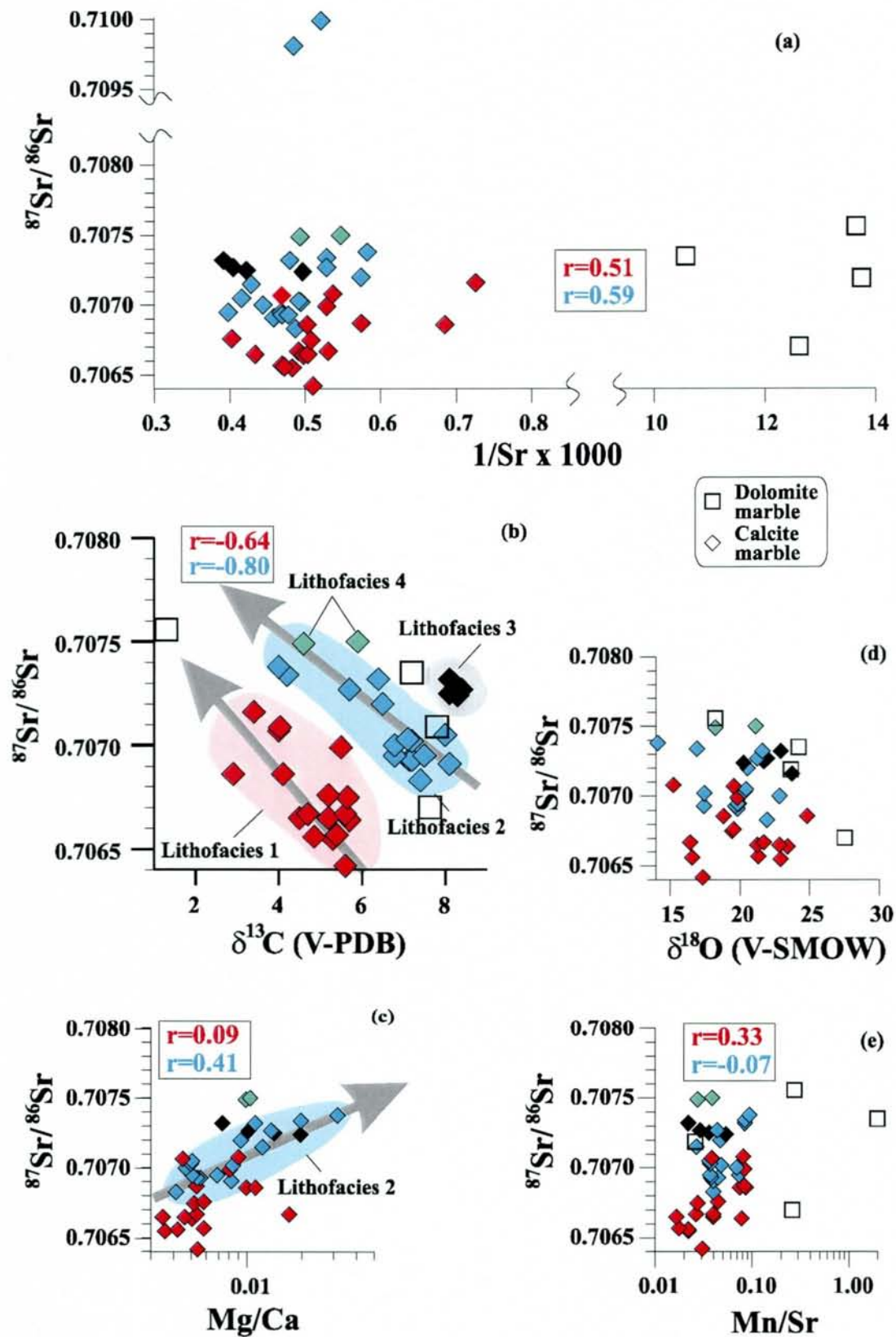


Figure 22. Strontium isotope ratios versus $\delta^{13}\text{C}$, $\delta^{18}\text{O}$, Mn/Sr, Mg/Ca and $1/\text{Sr}$ values. Pink- and blue-shaded areas as well as grey arrows indicate alteration trends.

of Sr concentration with correlation coefficient of 0.51 and 0.59, respectively (Fig. 22a). This suggests that the selected samples may still include those subjected to alteration, which caused resetting of the strontium isotope system.

Strontium isotope ratios plotted against $\delta^{13}\text{C}$, $\delta^{18}\text{O}$ as well as Mn/Sr and Mg/Ca ratios (Fig. 22b-d) reveal clear alteration trends. For Lithofacies 1 and 2 this is exemplified by a strong negative covariation between the strontium and carbon isotopes (Fig. 22b). Lithofacies 2 clearly demonstrates that enrichment in ^{87}Sr is related to dolomitisation (Fig. 22c). Thus, the discrimination diagrams all together (Fig. 21, 22) indicate that dolomitisation was the major process which affected carbon, oxygen and strontium isotope systems. Dolomitisation introduced Mn and radiogenic strontium, and depleted carbonates in ^{13}C , ^{18}O and Sr. We exclude from further consideration those samples of Lithofacies 1 and 2 which are plotted on $^{87}\text{Sr}/^{86}\text{Sr}$ versus $\delta^{13}\text{C}$ diagram outside of the tightly clustered groups (Fig. 22b), as well as samples with $1/\text{Sr} < 0.6$ (Fig. 22a). All the samples excluded from further applications are marked in Table 2 in italics. The other remaining 26 samples will be denoted in the subsequent discussion as the 'least altered' or the 'best preserved' population. They are indicated in Table 2 by bold-face letters.

The retained 26 samples represent the four lithofacies which are also recognised as four lithostratigraphic units (Fig. 2):

1. Ten samples from Lithofacies 1 have the $\delta^{13}\text{C}$ values ranging from +4.5‰ to +5.7‰ averaging at +5.2 ± 0.4‰. The $\delta^{18}\text{O}$ range is 19.9-22.9‰ with the average value of 19.9 ± 2.5‰. The range of the $^{87}\text{Sr}/^{86}\text{Sr}$ values is 0.70642-0.70676 with the average at 0.70662 ± 0.00010.

2. Eleven samples from Lithofacies 2 are characterised by the $\delta^{13}\text{C}$ values ranging from +6.5‰ to +8.1‰ averaging at 7.2 ± 0.5‰, and the $\delta^{18}\text{O}$ values varying from 17.4‰ to 22.8‰ with the average value at 20.0 ± 1.6‰. The range of the $^{87}\text{Sr}/^{86}\text{Sr}$ values is 0.70683-0.70720 with the average at 0.70698 ± 0.00010.

3. Four samples from Lithofacies 3 show a narrow range of high $\delta^{13}\text{C}$ and $\delta^{18}\text{O}$ values from +8.1‰ to 8.4‰ and from 20.2‰ to 22.9‰, respectively. The $^{87}\text{Sr}/^{86}\text{Sr}$ values range from 0.70724 to 0.70732.

4. The two samples from Lithofacies 4 are marked by the intermediate $\delta^{13}\text{C}$ and $\delta^{18}\text{O}$ values of 4.6-5.9‰ and 18.2-21.1‰, respectively. The $^{87}\text{Sr}/^{86}\text{Sr}$ ratios are the highest of all, ranging from 0.70749 to 0.70750.

Although we concluded that post-sedimentary processes caused depletion of marbles in ^{13}C one may argue that the highly positive $\delta^{13}\text{C}$ values might also have been developed through either metamorphic devolatilisation or during diagenesis instead of being primary depositional signatures. The possibility that the ^{13}C -rich carbonates formed from metamorphic devolatilisation of a low- ^{13}C , methane-rich fluids is unlikely as methane-rich fluids are very uncommon during metamorphism. The available mineral assemblages do not suggest such fluids. Meteoric and non-fermentative diagenesis typically shifts both oxygen and carbon isotopes towards lower values in (e.g., Hudson 1977). Fermentative diagenesis usually occurs under anaerobic conditions and starts at depth as soon as sulphate reduction stops (Irwin et al. 1977). The transformation of buried organic matter results in the generation of CH_4 depleted in ^{13}C (down to -70‰) and isotopically heavy CO_2 ($\delta^{13}\text{C}$ perhaps up to +15‰). Consequently, isotopically heavy carbon dioxide produced in this process may result in ^{13}C -rich carbonate deposition. However, CH_4 may be also oxidised to CO_2 . The latter can be contributed to HCO_3^{2-} and form carbonates depleted in ^{13}C . Therefore carbonate minerals precipitated in the course of fermentative diagenesis may show a wide range in $\delta^{13}\text{C}$, though the temperature dependent oxygen isotope ratios will show very little variation (e.g., Watson et al. 1995), which is not seen in Figure 20.

11. THE APPARENT AGE OF THE SOKUMFJELL GROUP

Previous researchers have not dated the Sokumfjell Group. The Rb-Sr whole-rock data obtained for pelitic schist of Habreså/Stabben and Vegdal units as well as for the Stabursdal gneiss (Fig. 3) cannot be considered alone as reliable ages. This is because interpretation of

Rb-Sr whole-rock dating of sedimentary and metasedimentary rocks is a difficult task. In general, there are always several options to be considered. For example, isotope homogenisation may occur during diagenesis (Perry & Turekian 1974) or low-grade metamorphism (Gebauer & Grünefelder 1974), or metamorphism does not result in isotopic homogenisation at all (e.g. Krogh & Davies 1973).

In general, dating of non-fossiliferous carbonates provides many problems regardless of their actual age. In recent years, temporal trends in carbon and strontium isotopes have been applied not only for stratigraphic correlation of Phanerozoic but also for the Proterozoic sequences. The concept of carbon and strontium isotope stratigraphy of Proterozoic carbonates has been gradually developed over the last 15 years (Veizer et al. 1983, Knoll et al. 1986, Asmeron et al. 1991, Knoll & Walter 1992, Derry et al. 1992, Kaufman et al. 1993, Gorokhov et al. 1995, Kaufman & Knoll 1995, Kuznetsov et al. 1997) and resulted in a reasonably well constructed $\delta^{13}\text{C}_{\text{carb}}$ and $^{87}\text{Sr}/^{86}\text{Sr}$ secular curves for seawater. However, the two $\delta^{13}\text{C}_{\text{carb}}$ reference curves, one by Derry et al. (1992), other by Kaufman & Knoll (1995) are inconsistent within 520-570 and 700-850 Ma time intervals. Additionally, the curve by Kaufman & Knoll (1995) have recently been seriously questioned by Kennedy et al. (1998). Therefore in subsequent age constraints we favour the $^{87}\text{Sr}/^{86}\text{Sr}$ secular curve.

In general, the carbonate rocks of the Northern and Central Norwegian Caledonides are poorly studied in terms of their isotopic composition. However, a few short communications have indicated the presence of carbonates of different age groups spanning from 520 to 640 Ma with very distinctive isotopic signatures (Trønnes & Sundvoll 1995, Melezhik et al. 1997, Melezhik et al. 1999). Thus, there is an indication that the chemostratigraphy could be applicable for high grade carbonate rocks of the Norwegian Caledonides.

11.1 Strontium isotope variations

The results suggest a progressive increase in $^{87}\text{Sr}/^{86}\text{Sr}$ values upwards in the tectonostratigraphic section (Fig. 23). If the average values, calculated from the least altered samples, are projected into the seawater curve (Fig. 24) the apparent depositional ages of the studied carbonates are tightly clustered between 597 and 608 Ma. Note that palaeoseawater trend shows an increase in radiogenic component with decreasing age, just exactly as it was

recorded for the terminal Proterozoic trend (Fig. 24). The obtained ages are in agreement with the previous Rb-Sr estimates of 858 Ma for the underlying Stabbursdal gneiss. However, the Sokumfjell carbonate ages are somewhat younger than 690 ± 63 , 658 ± 29 Ma obtained by Rb-Sr

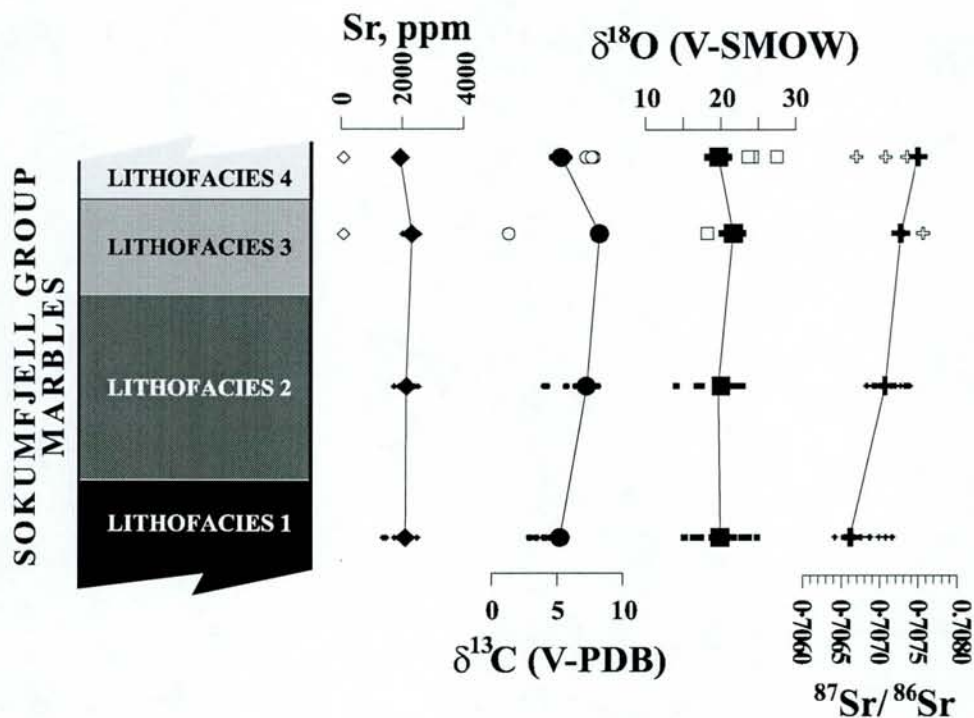


Figure 23. Stratigraphic variation of $^{87}\text{Sr}/^{86}\text{Sr}$, $\delta^{13}\text{C}$ and $\delta^{18}\text{O}$ in carbonates of the Sokumfjell Group. Mean values, indicated as large symbols, are based on the least altered samples (Table 2, see text). Ranges, indicated by small solid symbols, are based on the least altered samples (Table 2). Values for dolomite marbles are indicated by open symbols.

whole-rock chronometer from the Kovdistind and Vegdal metapelites, respectively (Tørudbakken & Brattli 1985, Styles 1978). Both these units are tectonostratigraphically above the Sokumfjell carbonates. Considering the chemistry of the studied samples, having Sr content above 2000 ppm, it is not believed that they can be shifted downwards to the level of 690-650 Ma. Instead, we suggest that the previous geochronological estimates based on aluminosilicate components in metapelites very likely reflect mixed ages due to the presence of older detrital phases which were not fully isotopically homogenised during diagenesis. Another, much younger, age of 606 ± 99 Ma obtained by Rb-Sr whole-rock chronometer from the same Kovdistind metapelite (Tørudbakken & Brattli 1985) proves this assumption. Alternatively, though less probable, the Kovdistind and Vegdal units are older than the Sokumfjell Group marbles.

7.2 Carbon isotope variations

The positive $\delta^{13}\text{C}_{\text{carb}}$ values of +5 to +8‰ obtained from the studied carbonates match those reported from Neoproterozoic succession elsewhere (Fig. 24). However, when the $\delta^{13}\text{C}_{\text{carb}}$ averages are projected into seawater curve the only Lithofacies 1 and 4 data match 600 Ma whereas other $\delta^{13}\text{C}_{\text{carb}}$ averages suggest older ages of 610-630 Ma. Note, that the Sokumfjell Group marbles show first an increase in ^{13}C with decreasing age (Fig. 23), opposite to the

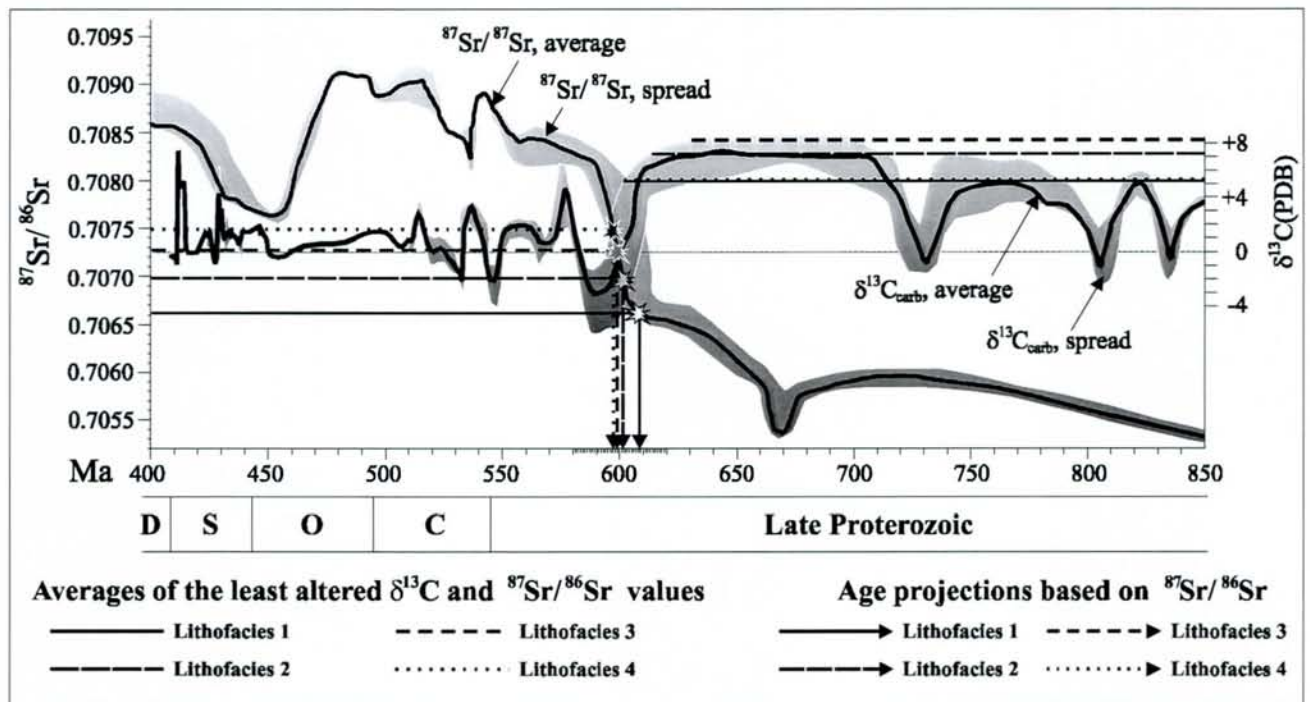


Figure 24. $^{87}\text{Sr}/^{86}\text{Sr}$ and $\delta^{13}\text{C}$ and $\delta^{18}\text{O}$ age curves with projections of mean $^{87}\text{Sr}/^{86}\text{Sr}$ and $\delta^{13}\text{C}$ values calculated from the least altered samples of the Sokumfjell Group. Vertical arrowhead lines indicate apparent depositional ages for different lithofacies. The Sr-isotope calibration curve is based on data from Veizer et al. (1983), Asmeron et al. (1991), Derry et al. (1992), Gorokhov et al. (1995), Kaufman & Knoll (1995), Nicholas (1996) and Denison et al. (1998). The C-isotope calibration curve is based on data from Derry et al. (1992, 1993), Kaufman & Knoll (1995) and Azmy et al. (1998). The new age for the Cambrian-Ordovician boundary is based on Davidek et al. (1998).

terminal Proterozoic trend (Fig. 24). The only possible explanation may be that the studied carbonates represent short term temporal oscillations that could not have been resolved in the compilations on which the $\delta^{13}\text{C}_{\text{carb}}$ calibration curve has been made. This problem has been acknowledged by Misi and Veizer (1998) when they applied chemostratigraphy to the

Neoproterozoic carbonates in Brazil. They emphasised that $\delta^{13}\text{C}_{\text{carb}}$ fluctuation in Phanerozoic and Recent carbonates at any given time is of order of 5‰ (e.g., Veizer 1997). However, the driving forces of this spread are not entirely understood. Thus, based on these facts we favour Sr-ages that indicate time interval of 597-608 Ma.

12. INCONSISTENCY BETWEEN THE MAP AND THE AGE DATA

The lithological unit 7, which comprises the oldest rocks, has on both sides a common boundary with unit 6. The reason for this is so far not fully understood. Some possible explanations are given here.

- 1) The southwestern part of unit 6, for some reason, may be older than unit 7, but this has not been detected by the isotope analyses. Accordingly, the entire succession could be younging towards the northeast.
- 2) There may be an early slide or thrust along the western boundary of unit 7, causing repetition of the beds. The inferred thrust must be older than or coeval with the F_1 deformation as it is folded by F_1 structures. There are no traces of such a thrust, but as marbles readily recrystallised during deformation and metamorphism, this possibility cannot be excluded.
- 3) Unit 7 may represent the core of a recumbent anticlinal F_1 fold. This fold must be an overturned anticline as the oldest rocks are found in the core. The sequence from Kakvika to the area just north of Tverrvika is situated on the inverted limb of the F_1 fold.

The northwestern part of unit 7 has not been sampled for chemical analyses. It is included in unit 7 only because of its resemblance to that unit. Along its eastern boundary there is a fine-grained mica schist (unit 8) that is not found anywhere else. Its thickness varies from 4 m up to 8 m. The fact that it is not found elsewhere along the 6/7 boundary could be explained by a continuous rock sequence that is younging from the intrusive rocks in the west to unit 8 south of Tarnesodden.

Other explanations could be: (i) unit 8 has not been deposited farther east, (ii) this same unit is thinning out in that direction, (iii) there is a thrust along unit 8.

13. POTENTIAL OF THE SOKUMFJELL GROUP CARBONATES FOR WHITE MARBLES

White calcite marbles are mainly associated with Lithofacies 1 and 3 (Fig. 2, Appendix 1 & 2). However, considering the limitation, which industrial requirements put on non-carbonate components, only the Lithofacies 1 marbles can be estimated as a potential candidate for industrial use. Given that SiO₂ content of 3 wt% is the maximum limit for the paper industry, the amount of pure, white calcite marbles appears to be very limited (Table 1) and spatially restricted within the southern part of the mapped area (Fig. 2, Appendix 1, 2). However, even if the reserves were satisfactorily large the major obstacle for practical utilisation of these marbles is the ubiquitous inclusions of granite and pegmatite veins, dikes and boudins (Fig. 14). As the amount of these inclusions is very large the extraction of marbles will be inevitably followed by their contamination. The spatial distribution of the inclusions is not controlled by any measurable factors and therefore cannot be predicted in the course of mining operation. The overall conclusions are negative and this part of the Beiarn area should not be recommended for future exploration for white, pure, calcite marble.

The mapped area covers only a part of the Sokumfjel marbles. Neither the top nor the base of the group has been mapped in detail. However, from the regional mapping of the late eighties (Solli 1990) it has been established that granitic and tonalitic intrusions, dikes and veins abundantly occur throughout the area.

14. DATA BASE

The computerised data base includes ca. 100 XRF analyses as well as 93 CaO and MgO acid-soluble. Forty-six $\delta^{13}\text{C}$, $\delta^{18}\text{O}$ and $^{87}\text{Sr}/^{86}\text{Sr}$ isotope measurements are also included into the database. All the samples are provided with UTM-coordinates and digitally connected to 1:5,000 digital lithological map (Appendix 1 & 2).

15. CONCLUSIONS



Figure 25. Granite inclusions in Lithofacies 3 marbles.

1. The 1:5, 000 mapping of ca. 1000 m-thick carbonate sequence belonging to the Sokumfjell Group (Beiarn Nappe Complex) in the Uppermost Allochthon of the Nordland Caledonides reveal four different lithofacies of calcite marbles and one composed of dolomite marble.
2. The calcite marbles exhibit different scale rhythmic bedding and textural grading indicating that carbonate material was redeposited by pelagic turbidite system in both proximal and distal facies.

3. More than 100 samples were analysed for major and trace elements, Mg and Ca acid-soluble, and 46 samples were analysed for $\delta^{13}\text{C}$, $\delta^{18}\text{O}$ and $^{87}\text{Sr}/^{86}\text{Sr}$. All calcite marbles are enriched in Sr averaging at 2000 ppm. The calcite marbles are characterised by $^{87}\text{Sr}/^{86}\text{Sr}$ ratios ranging between 0.70642 and 0.70999, and $\delta^{13}\text{C}$ values ranging between +1.3 and +8.4‰ PDB. The 'best preserved' samples selected on the basis of their $\delta^{18}\text{O}$ values, and Mn and Sr concentration as well as their ratios, yield average $^{87}\text{Sr}/^{86}\text{Sr}$ values of 0.70662, 0.70698, 0.70727 and 0.70749 for Lithofacies 1, 2, 3 and 4, respectively.

4. Projection of the best preserved into $^{87}\text{Sr}/^{86}\text{Sr}$ and $\delta^{13}\text{C}$ values into $^{87}\text{Sr}/^{86}\text{Sr}$ and $\delta^{13}\text{C}$ calibration curves for the secular variations of seawater suggests that the lithofacies studied were apparently deposited within a 597-608 Ma time interval.
5. White, pure, calcite marbles of Lithofacies 1 were deposited at about 608 Ma. They have low contents of SiO_2 and MgO and can meet the requirements for industrial use. However, industrial extraction of pure marbles is hardly possible due to inevitable contamination by ubiquitous granite inclusions.
6. The studied area should not be considered for further exploration for white calcite marbles.
7. A computerised data base for the study includes more than 100 chemical and 46 isotope analyses connected to 1:5,000 digital lithological map.

References

- Azmy, K., Jveizer, J., Basset, M.G. & Cooper, P. 1998: Oxygen and carbon isotopic composition of Silurian Brachiopods: Implications for coeval seawater and glaciations. *Geological Society of America Bulletin*, 110, 1499-1512.
- Bennett, J.D. 1970: The structural geology of the Saura region, Nordland. Norges geologiske undersøkelse No 264.
- Brand, U. & Veizer, J. 1980: Chemical diagenesis of multicomponent carbonate system - 1. Trace elements. *Journal of Sedimentary Petrology*, 50, 1219-1250.
- Brattli, B. & Tørudbakken, B., 1987: Berggrunnskart ARSTADDAL 2028 IV, M. 1:50 000. Norges geologiske undersøkelse.
- Asmeron, Y., Jacobsen, S.B. Knoll, A.H., Butterfield, N.J. & Swett, K. 1991: Strontium isotopic variations of Neoproterozoic seawater: Implications for crustal evolution. *Geochimica et Cosmochimica Acta* 55, 2883-2894.
- Cook and Enos, P. (Eds.), 1977: Deep-Water Carbonate Environments. SEPM Special Publication, 25, 336 pp.
- Cook, H.E. & Mullins, H.T., 1983: Basin margin environments. In: Scholle, P.A., Bebout, D.G. & Moore, C.H. (Eds.) *Carbonate Depositional Environments*. American Association of Petroleum Geologists, Tulsa, Oklahoma 74101, USA, pp. 539-617.
- Davidek, K., Landing, E., Bowring, S.A., Westrop, S.R., Rushton, A.W.A., Fortey, R.A. & Adrain, J.M., 1998: New uppermost Cambrian U-Pb date from Avalonian Wales and age of the Cambrian–Ordovician boundary. *Geological Magazine*, 135(3), 305-309.
- Denison, R.E., Koepnick, R.B., Burke, W.H. & Hetherington, E.A., 1998: Construction of the Cambrian and Ordovician seawater $^{87}\text{Sr}/^{86}\text{Sr}$ curve. *Chemical Geology*, 152, 325-340.

Derry, L.A., Kaufman, A.J. & Jacobsen, S.B., 1992. Sedimentary cycling and environmental changes in the Late Proterozoic: Evidence from stable and radiogenic isotopes. *Geochimica et Cosmochimica Acta*, 56, 1317-1329.

Einsele, G., Ricken, W. & Seilacher, A., 1991: Cycles and events in stratigraphy—basic concept and terms. In: Einsele, G., Ricken, W. & Seilacher, A. (Eds.), *Cycles and Events in Stratigraphy*, Springer-Verlag Berlin Heidelberg, pp. 1-19.

Fairchild, I.J., Marshall, J.D. & Bertrand-Sarafati, J., 1990. Stratigraphic shifts in carbon isotopes from Proterozoic stromatolitic carbonates (Mauritania): Influences of primary mineralogy and diagenesis. *American Journal of Science*, 290-A, 46-79.

Gebauer, D & Grünenfelder, M., 1974: Rb-Sr whole-rock dating of late diagenetic to anchimetamorphic, Palaeozoic sediments in Southern France (Montagne Noire). *Contribution to Mineralogy and Petrology* 47, 113-130.

Gorokhov, I.M., Semikhatov, M.A., Baskakov, A.B., Kutuyavin, E.P., Mel'nikov, N.N., Sochava, A.V. & Turchenko, T.L. 1995: Strontium isotope composition in Riphean, Vendian and Lower Cambrian carbonates. *Stratigraphy and Geological Correlation* 3 (1), 3-33.

Cribb, J.S., 1981: Rb-Sr geochronological evidence suggesting a reinterpretation of part of the north Norwegian Caledonides. *Norsk geologisk tidsskrift* 61, 97-110.

Guerrera, A., Peacock, S.M., Knauth, L.P., 1997. Large ^{18}O and ^{13}C depletion in greenschist facies carbonate rocks, western Arizona. *Geology* 25, 943-946.

Hollingworth, S.E., Wells, M.K. & Bradshaw, R., 1960: Geology and structure of the Glomfjord Region, N. Norway. *Proceedings of the International Geological Congress* 21(19), 33-42.

Hudson, J.D., 1977: Stable isotopes and limestone lithification. *Journal of the Geological Society of London* 133, 637-660.

- Irwin, H., Curtis, C., Coleman, M., 1977. Isotopic evidence for source of diagenetic carbonates formed during burial of organic-rich sediments. *Nature* 260, 209-213.
- Kaufman, A.J & Knoll, A.H. 1995: Neoproterozoic variations in the C-isotopic composition of seawater: stratigraphic and biogeochemical implications. *Precambrian Research* 73, 27-49.
- Kaufman, A.J., Jacobsen, S.B. & Knoll, A.H. 1993: The Vendian record of Sr and C isotopic variations in seawater: Implications for tectonics and paleoclimate. *Earth & Planetary Science Letters* 120, 409-430.
- Kaufman, A.J., Knoll, A.H. & Awramik, S.M. 1992: Biostratigraphic and chemostratigraphic correlation of Neoproterozoic sedimentary successions: Upper Tindir Group, northwestern Canada, as a test case. *Geology* 20, 181-185.
- Kennedy, M.J., Runnegar, B., Prave, A.R., Hoffmann, K.-H. & Arthur, M.A., 1998: Two of four Neoproterozoic glaciations? *Geology* 26, 1059-1063.
- Knoll, A.H. & Walter, M.R., 1992. Latest Proterozoic stratigraphy and Earth history. *Nature* 356, 104-132.
- Knoll, A.H., Hayes, J.M., Kaufman, A.J., Swett, K. & Lambert, L.B., 1986. Secular variations in carbon isotope ratios from upper Proterozoic successions of Svalbard and East Greenland. *Nature* 321, 832-838.
- Krogh, T.E. & Davies, G.L., 1973: The effect of regional metamorphism on U.Pb system in zircon and a comparison with Rb-Sr system in the same whole rock and its constituent minerals. *Yearbook Carnegie Institute Washington*, 72, 601-610.
- Kuznetsov, A.B., Gorokhov, I.M., Semikhatov, Melnikov, N.N., Kozlov, V.I., 1997: Strontium isotope composition in limestones of the Inzerskaya Formation, the Upper Riphean stratotype of the Southern Urals. *Transaction of the Academy of Sciences, Section Geochemistry* V.353, No.2, 249-254. (in Russian).

- McCrea, J.M., 1950: On the isotopic chemistry of carbonates and a paleotemperature scale. *Journal of Chemical Physics* 18, 849-857.
- Melezhik, V.A, Roberts, D., Pokrovsky, B.G., Gorokhov, I.M. & Ovchinnikova G.V., 1997: Primary isotopic features in metamorphosed Caledonian carbonates: implications for depositional age. (Extended abstract). *Norges geologiske undersøkelse Bulletin* 433, 22-23.
- Misi, A. & Veizer, J., 1998: Neoproterozoic carbonate sequences of the Una Group, Irecó Basin, Brasil: chemostratigraphy, age and correlations. *Precambrian Research*, 89, 87-100.
- Nicholas, C.J., 1996: The Sr isotopic evolution of the oceans during the 'Cambrian Explosion'. *Journal of the Geological Society of London*, 153, 243-254.
- Perry, E.-A., Jr. & Turekian, K.K., 1974: The effect of diagenesis on the redistribution of strontium isotopes in shales. *Geochimica et Cosmochimica Acta* 36, 929-935.
- Rosenbaum, J. M. & Sheppard, S.M.F., 1986: An isotopic study of siderites, dolomites and ankerites at high temperatures. *Geochimica et Cosmochimica Acta*. 50, 1147-1159.
- Rutland, R.W.R., 1959: Structural geology of the Sokumvatn area, North Norway. *Norsk geologisk tidsskrift* 39, 287-337.
- Rutland, R.W.R. & Nicholson, R., 1965: Tectonics of the Caledonides of part of Nordland, Norway. *Quart. J. Geol. Soc., London*, 121, 73-109.
- Scholle, P.A., Arthur, M.A. & Ekdale, A.A., 1983: Pelagic environments. In: Scholle, P.A., Bebout, D.G., Moore, C.H. (Eds.) *Carbonate Depositional Environments*. American Association of Petroleum Geologists, Tulsa, Oklahoma 74101, USA, pp. 619-691.
- Seilacher, A. & Aigner, T., 1991: Storm deposition at the bed, facies, and basin scale. In: Einsele, G., Ricken, W. & Seilacher, A. (Eds.), *Cycles and Events in Stratigraphy*, Springer-Verlag Berlin Heidelberg, pp. 249-267.
- Solli, A., 1990: SALTSTRAUMEN 2029 III, berggrunnskart M 1:50 000. Norges geologiske undersøkelse.

Styles, M.T., 1974: The structure, metamorphism and igneous petrology of the Beiarn area, Nordland, North Norway. *Unpubl. Ph.D. thesis*, Univ. of Manchester.

Styles, M. T., 1978: The structure, metamorphism and geochronology of the Beiarn region, Nordland and its tectonic implications. *In* Cooper, M.A. & Garton, M.R. (eds) *Tectonic Evolution of the Scandinavian Caledonides*. City of London Polytechnic

Trønnes, R.G. & Sundvoll, B., 1995. Isotopic composition, depositional ages and environments of Central Norwegian Caledonian marbles. (Extended abstract). *Norges geologiske undersøkelse Bulletin 427*, 44-47.

Tørudbakken, B.O. & Brattli, B. 1985: Ages of metamorphic and deformational events in the Beiarn Nappe Complex, Nordland, Norway. *Norges geologiske undersøkelse Bull.* 399, 27-39.

Veizer, J., Compston, W., Clauer, N. & Schidlowski, M. 1983: $^{87}\text{Sr}/^{86}\text{Sr}$ in Late Proterozoic carbonates: evidence for a 'mantle' event at ~900 Ma ago. *Geochimica et Cosmochimica Acta* 47, 295-302.

Watson, R.S., Trewin, N.H. & Fallick, A.E., 1995: The formation of carbonate cement in the Forth and Balmoral Fields, northern North Sea: a case for biodegradation, carbonate cementation and oil leakage during early burial. *In*: Harley, A.J. & Prosser, D.J. (Eds.), *Characterization of Deep Marine Clastic Systems*, Geological Society Special Publication 94, 177-200.

Wilson, J.L., 1969: Microfacies and sedimentary structures in 'deeper water' lime mudstone. *In*: Friedman, G.M. (Ed.) *Depositional Environments in Carbonate Rocks*. SEPM Special Publication, 14, 4-19.

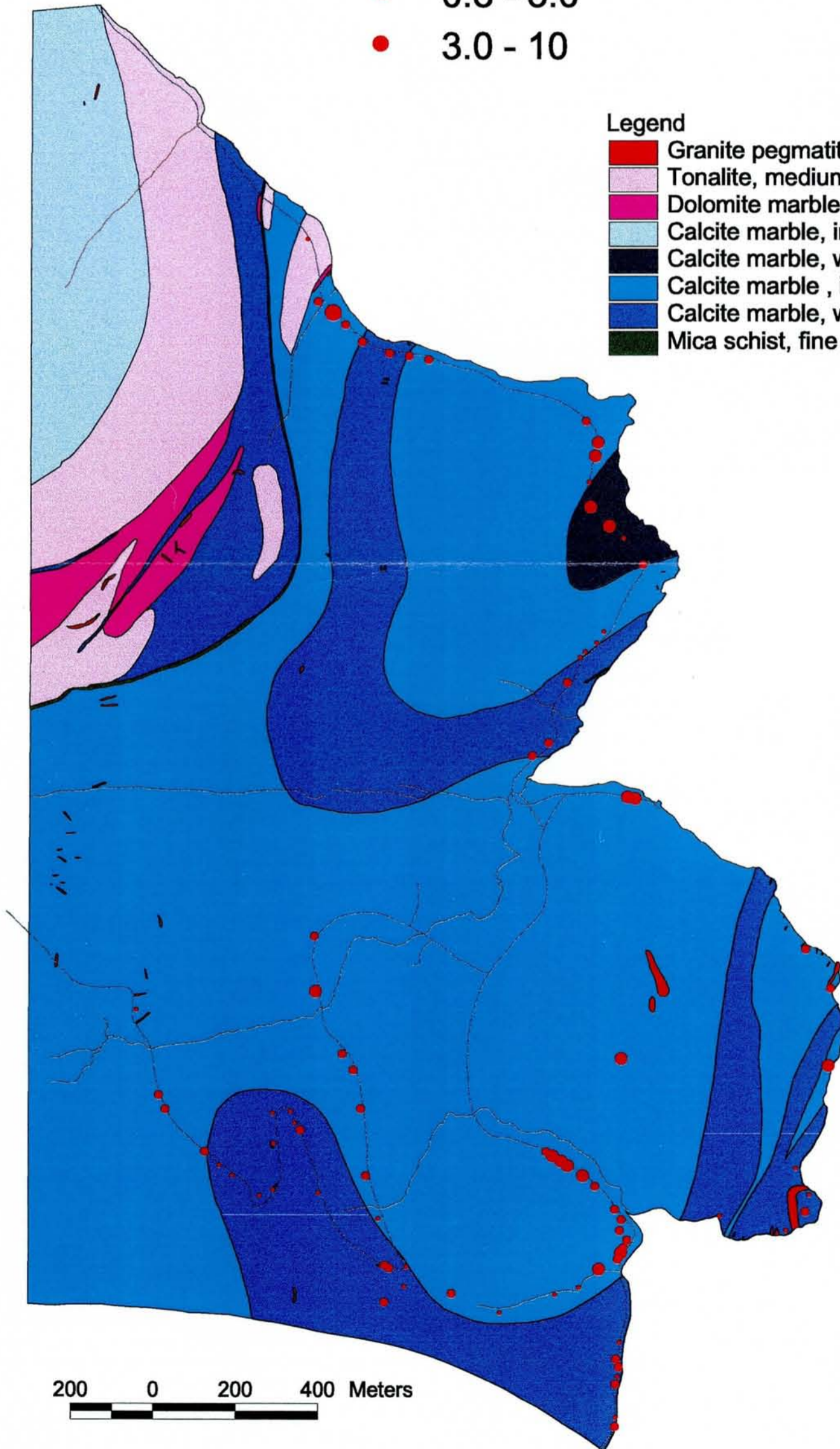
Variation in acid soluble MgO, wt%

- 0 - 0.4
- 0.4 - 0.8
- 0.8 - 3.0
- 3.0 - 10



Legend

- Granite pegmatite, white
- Tonalite, medium-grained
- Dolomite marble, white, medium-grained
- Calcite marble, impure, pale grey
- Calcite marble, white, medium-grained, banded
- Calcite marble, impure, grey, thin beds of schists
- Calcite marble, white, rhythmically bedded
- Mica schist, fine grained and rusty



200 0 200 400 Meters

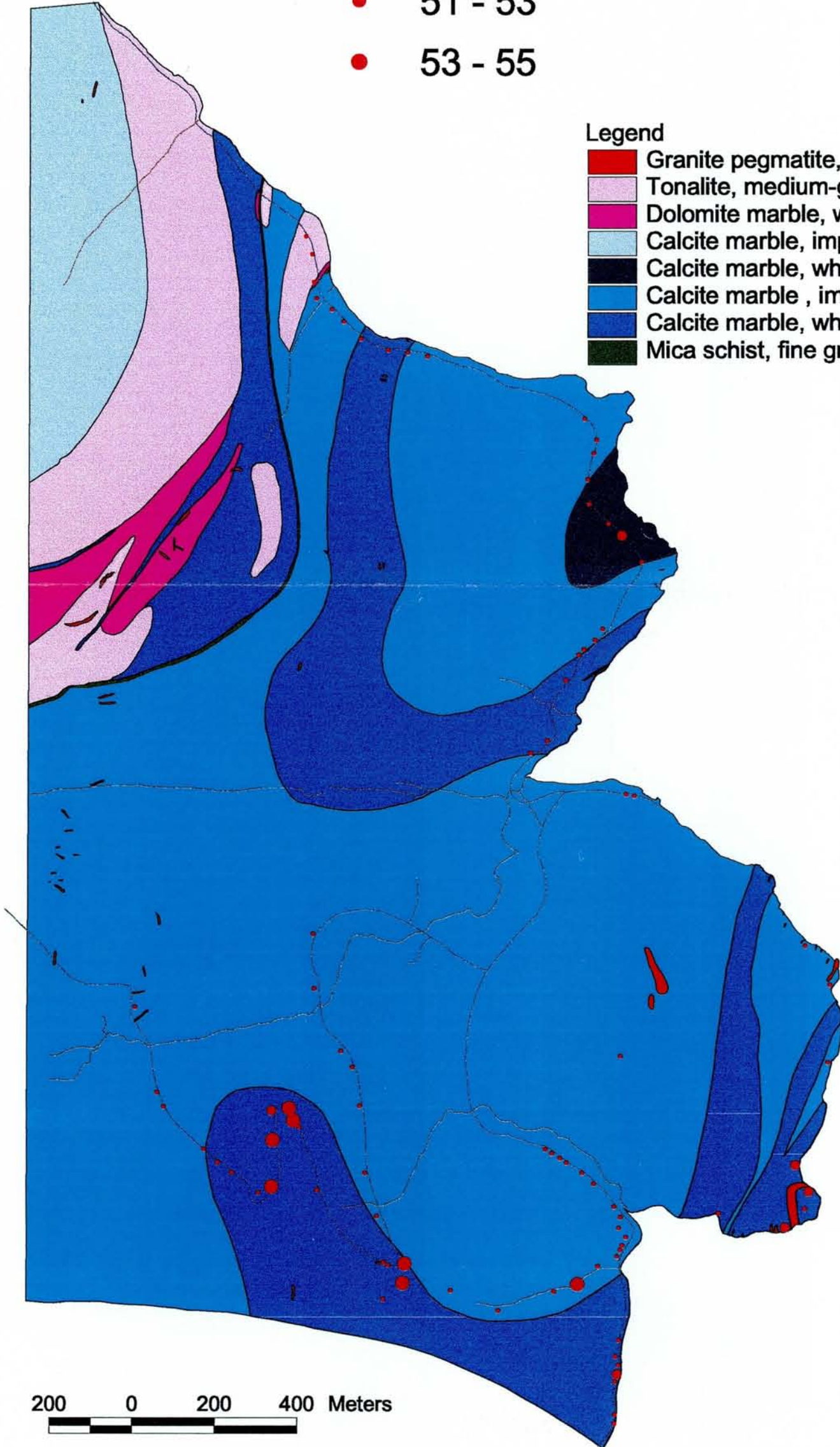
Variation in acid soluble CaO, wt %



- 0 - 51
- 51 - 53
- 53 - 55

Legend

- Granite pegmatite, white
- Tonalite, medium-grained
- Dolomite marble, white, medium-grained
- Calcite marble, impure, pale grey
- Calcite marble, white, medium-grained, banded
- Calcite marble, impure, grey, thin beds of schists
- Calcite marble, white, rhythmically bedded
- Mica schist, fine grained and rusty



200 0 200 400 Meters